

Recent Advances in Superparamagnetic Iron Oxide Nanoparticles for Cellular Imaging and Targeted Therapy Research

Yi-Xiang J. Wang^{1,2,*}, Shouhu Xuan³, Marc Port⁴ and Jean-Marc Idee⁴

¹Department of Imaging and Interventional Radiology, The Chinese University of Hong Kong, Prince of Wales Hospital, Shatin, New Territories, Hong Kong SAR, China; ²Guangdong Medical College the Shenzhen No. 3 People's Hospital, Shenzhen 518020, China; ³CAS Key Laboratory of Mechanical Behavior and Design of Materials, Department of Modern Mechanics, University of Science and Technology of China, Hefei 230026, China; ⁴Research Division, Guerbet, BP57400, 95943 Roissy CDG Cedex, France

Abstract: Advances of nanotechnology have led to the development of nanomaterials with both potential diagnostic and therapeutic applications. Among them, superparamagnetic iron oxide (SPIO) nanoparticles have received particular attention. Over the past decade, various SPIOs with unique physicochemical and biological properties have been designed by modifying the particle structure, size and coating. This article reviews the recent advances in preparing SPIOs with novel properties, the way these physicochemical properties of SPIOs influence their interaction with cells, and the development of SPIOs in liver and lymph nodes magnetic resonance imaging (MRI) contrast. Cellular uptake of SPIO can be exploited in a variety of potential clinical applications, including stem cell and inflammation cell tracking and intra-cellular drug delivery to cancerous cells which offers higher intra-cellular concentration. When SPIOs are used as carrier vehicle, additional advantages can be achieved including magnetic targeting and hyperthermia options, as well as monitoring with MRI. Other potential applications of SPIO include magnetofection and gene delivery, targeted retention of labeled stem cells, sentinel lymph nodes mapping, and magnetic force targeting and cell orientation for tissue engineering.

Keywords: Superparamagnetic, iron oxide nanoparticles, SPIO, cell labeling, surface coatings, MRI, targeted drug delivery, magnetic targeting, hyperthermia.

1. INTRODUCTION

Among all types of nanoparticles, biocompatible superparamagnetic iron oxide (SPIO) nanoparticles with proper surface architecture attracted extensive attention for both cellular imaging and drug delivery applications. Key features of SPIOs include their ability to exhibit magnetization only in an applied magnetic field; their ability to form stable colloidal suspensions which is crucial for biomedical applications, especially *in vivo*; they induce faster T₂/T₂* relaxation and such can be utilized as MRI contrast agent; and that they can be directed to a desired site in the body by a magnetic force, making them useful for controlled targeting clinically. Desirable SPIO features also include the ability to control their size and size distribution, a uniform shape, strong magnetic susceptibility and the desired surface chemistry. In the past few years, extensive work has been done on synthesis and surface modification of SPIOs to yield desirable properties for biomedical applications. Monodispersed iron oxide particles with uniform size and shape, and high magnetization properties are of particular interest. Tailored surface engineering of the particles can be done through creating a polymeric or inorganic molecular shell surrounding the iron oxide cores, followed by the functionalization with specific biomolecules on the outer shell layer [1].

The clinical applications of SPIO include MR contrast imaging for liver tumor and lymph nodes metastasis [2-4]. SPIOs have important potentials for *in vivo* stem cell tracking [5-6], magnetic separation [7], hyperthermia therapy [8], and anticancer drug delivery [9-11]. Therapeutic and diagnostic agents can be encapsulated, covalently attached, or adsorbed onto nanoparticles. In the mesoscopic size range of 5-100 nm diameter, nanoparticles possess large surface areas for conjugating to multiple diagnostic and therapeutic agents. Multi-pore nanoshells are also used for encapsulating

drugs. For many of these applications, optimized cellular uptake of SPIO nanoparticles by target cells is a critical step. One strategy to modulate the cellular uptake efficiency or specificity of SPIO nanoparticles is to modify their surface coating [1, 9, 12]. Nanoparticles facilitated drug delivery offers higher intra-cellular concentration. When SPIO nanoparticles are used as carrier vehicle, additional advantages are achieved including magnetic targeting and hyperthermia options, as well as visualization with magnetic resonance imaging (MRI).

This article covers the recent advances in preparing SPIOs with novel properties, how the physicochemical properties of SPIO will influence their efficiency of cell labeling, and how cellular uptake of SPIOs can be exploited in clinical applications, including stem cell and inflammation cell tracking, and intra-cellular drug delivery to cancerous cells. The development of SPIOs in liver and lymph nodes MRI contrast together is discussed. This article also reviews a number of potential applications of SPIOs, including magnetic targeting, hyperthermia, magnetofection and gene delivery, targeted retention of labeled stem cells, sentinel lymph nodes mapping and magnetic force targeting and cell orientation for tissue engineering.

2. PREPARATION OF SPIO NANOPARTICLES

The physical and chemical properties of magnetic particles are highly influenced by their size, shape, crystallinity and surface characteristics. When the particle size is decreased to the critical value r_c , the magnet changes from a multiple domains state to a single domain state [13]. In this case, the magnetic nanoparticle is just like a giant paramagnetic atom and responses fast to the external magnetic field. After the removal of the external magnetic field, a negligible residual magnetization and coercivity will be found, and this kind of magnetic nanoparticles is superparamagnetic.

Aqueous co-precipitation is the most commonly used method for SPIO fabrication due to the simplicity of this synthesis and the possibility to obtain large quantity of nanoparticles in smooth manufacturing conditions. In 1925, Welo *et al.* firstly reported this approach [14]. By adding a base solution (sodium hydroxide or ammonium) into the aqueous Fe²⁺/Fe³⁺ solution under an inert at-

*Address correspondence to this author at the Department of Imaging and Interventional Radiology, The Chinese university of Hong Kong, Prince of Wales Hospital, Shatin, New Territories, Hong Kong SAR, China; Tel: (852) 2632 2289; Fax: (852) 2636 0012; E-mail: yixiang_wang@cuhk.edu.hk

mosphere, water dispersible SPIO nanoparticles can be obtained. The size, shape, composition, and surface nature can be controlled by varying the type of the iron salt, the $\text{Fe}^{2+}/\text{Fe}^{3+}$ ratio, the reaction temperature, the pH value, and the surfactants [15]. The surface status of SPIOs can be controlled by adding surfactants or polymers during the preparation. If oleic acid is introduced in the reaction, the obtained SPIOs exhibit a hydrophobic nature and can well disperse into the organic solvent [16]. Most of SPIOs reported in the literature are used in the biomedical field, thus various biopolymers such as dextran, alginate, protein, polyethylene glycol (PEG), polyacrylic acid (PAA), poly (vinyl alcohol) (PVA) and polyethyleneimine (PEI) are used as the coating reagents. These polymers can be adsorbed onto the surface of SPIOs where they act as the stabilizing agent to form stable aqueous solution. The nucleation of SPIOs occurs in the presence of the polymers, thus the adsorbed polymers can inhibit the growth of the nanoparticles and lead to the small size. Moreover, the polymers can also slow down the growth rate of the nuclei, which favors the formation of monodispersed SPIO nanocrystals. Other SPIO synthesis uses monomeric stabilizers as coating agents such as carboxylates, phosphates or sulfates [17].

The magnetic saturation value (M_s) of SPIO nanocrystals is usually not optimal due to the imperfect crystallization of the SPIO nanocrystals obtained through a method with low temperature and pressure. Therefore, the hydrothermal treatment is applied to improve the crystallization of SPIO nanocrystals. Wang *et al.* developed a one-step hydrothermal method to synthesize well crystallized SPIO nanoparticles by using ferrous chloride and diamine hydrate as the starting materials [18]. The sample prepared at 140 °C exhibits a saturation magnetization of 85.8 emu/g while, the 100 °C reaction leads to a value of 12.3 emu/g. With increasing of the temperature, the crystallite size for mono-domain nanocrystal increases, which further leads to the increase of the M_s . To improve the dispersability of SPIO nanoparticles, Xuan *et al.* reported a facile hydrothermal method to synthesize water dispersible SPIO nanocrystals [19]. The ascorbic acid is applied both as the reducing reagent and the capping ligand, where the Fe^{3+} is in situ reduced to form SPIOs and the oxidized ascorbic acid is capped onto the surface of SPIOs. Similarly, hydrophobic SPIO nanoparticles can also be synthesized by using the solvothermal method. Via the reaction between Fe powder and ferric chloride, monodispersed SPIO nanocrystals can be obtained in n-hexane solvent in the presence of oleic acid and laurylamine [20]. The as-prepared SPIO nanocrystals are homogeneously dispersed within the hexane solvent and the solution remains stable for weeks at room temperature. The average size is tunable from 5.2 to 12.7 nm by varying the reaction time and the M_s value can reach as high as 84 emu/g. Moreover, this method can also be extended to synthesize other kinds of SPIOs using Fe-complex as the single iron precursor [21].

The thermal decomposition approach was first employed to synthesize high-quality semiconductor nanocrystals [22, 23]. Inspired by this method, Sun *et al.* reported the fabrication of monodispersed SPIO nanocrystals by thermal decomposition method in 2002 [24]. Under high temperature, the iron acetylacetonate decomposes to form uniform SPIO nanoparticles in phenyl ether in the presence of alcohol, oleic acid, and oleylamine. With this method, large SPIO nanoparticles can also be synthesized using the small SPIO nanoparticles as seeds with the size ranging from 4 to 16 nm. Moreover, the $\text{Fe}(\text{CO})_5$ and metal fatty acid salts can also be used for the preparation of monodispersed SPIO nanocrystals. Park *et al.* found that this method is effective and productive, and has the ability to produce SPIO nanoparticles at tens of grams scale [25]. The results indicate that the size of the SPIO nanoparticles can effectively be controlled by varying the reaction temperature. In 2005, Park *et al.* further reported the method for one-nanometer-scale size-controlled synthesis of the monodispersed SPIO nanoparticles, in which the size depends on the initial iron nanoparticle seeds and iron oleate solutions [26]. Unfortunately, all of the above

SPIO nanoparticles cannot directly disperse into aqueous solution due to their long alkyl chain surfactant coating and can only dissolve in the non-polar solvent. To solve this problem, Li *et al.* developed a novel thermal decomposition method to produce water-dispersible SPIO nanoparticles where the strongly polar 2-pyrrolidone solvent is used [27]. By using the $\text{Fe}(\text{acac})_3$ as the iron source, water-dispersible SPIO nanoparticles are obtained and the size can be controlled from 5 to 11 nm by using the seeding method. To greener the synthesis, only ferric chloride is applied in a new approach and the results are promising [28]. The uniform SPIO nanocrystals can be obtained by simply boiling the 2-pyrrolidone solution of ferric chloride, and the size is controllable by varying the reaction time.

Due to their strongly size-dependent properties, size controllable synthesis of SPIO nanoparticles is highly desirable. By pyrolyzing the iron fatty acid precursor, monodispersed SPIO nanocrystals have successfully been obtained and the sizes range from 6 nm to 50 nm [29]. By introducing HOOC-PEG-COOH into the $\text{Fe}(\text{acac})_3$ -phenyl ether-oleylamine system, the size of SPIO nanoparticles can be controlled between 19 to 42 nm. Recently, Ge *et al.* developed a high-temperature solution-phase process to synthesize monodispersed SPIO nanoparticles, where ferric chloride is used as the iron precursor and diethylene glycol as a solvent [30]. The average size of the as-prepared SPIO is tunable between 30 to 180 nm by simply changing the NaOH concentration. These SPIO particles exhibit a cluster nanostructure and are composed of small primary magnetite nanocrystals, which render their superparamagnetic characteristic. Due to the presence of the polyacrylic acid chains in the cluster, the SPIO particles are water dispersible. With increasing of the cluster size, the M_s value increases and large SPIO particles respond to the external magnetic field much quicker than small SPIO nanocrystals. Solvothermal method has been proven to be another effective approach for controlling the size of SPIO particles. Deng *et al.* reported a modified reduction reaction between ferric chloride and ethylene glycol in a weak base medium system to produce monodisperse SPIO particles [31]. All the particles are uniformly dispersed and the size ranges from 200 to 800 nm, where the size is dependent on the reaction time. Inspired by this method, Liu *et al.* synthesized highly water-dispersible biocompatible SPIO microparticles using biocompatible trisodium citrate as an electrostatic stabilizer [32]. The size of the particles is tunable from 170 to 300 nm by varying the initial ferric chloride concentrations. However, controlling of SPIO particle size within 200 nm by using the solvothermal method still remains a challenge. To solve this problem, Xuan *et al.* developed a novel bi-solvent solvothermal reaction to construct monodispersed SPIO clusters. In this bi-solvent solvothermal reaction, the size of the SPIO cluster is rationally controlled between 10 to 280 nm by turning the volume ratio of ethylene glycol to diethylene glycol [33]. Interestingly, the primary grain size of the SPIO cluster is also tunable and ranges from 5.9 to 13.5 nm through varying the sodium acrylate/sodium acetate ratio. Moreover, by controlling the reaction parameter, both the ferromagnetic and superparamagnetic magnetite with tunable size can be obtained (Fig. 1) [34].

Apart from the above mentioned synthetic route, many other methods such as the microemulsion, ultrasonic solvothermal and H_2 reduction method are also effective [35-37]. In recent years, attention has also been paid to the preparations of SPIO particles with different morphologies such as rod, spindle, hollow sphere, porous sphere etc. [37-42].

3. SURFACE MODIFICATION OF SPIO NANOPARTICLES

There are several advantages in modifying the surface of naked SPIOs. Firstly, the stability of SPIO is a critical issue for their practical applications. Due to the high surface energy and the magnetic force, naked SPIOs can not uniformly disperse in aqueous solution without agglomeration or precipitation. Secondly, since Fe_3O_4 and

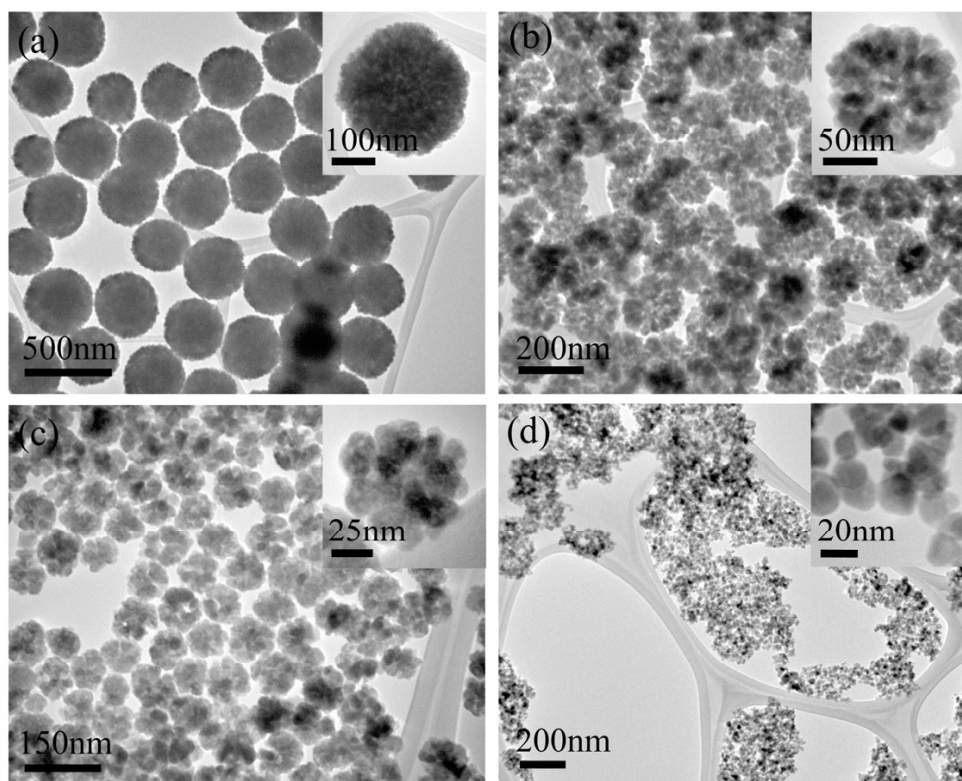


Fig. (1). TEM images of the Fe_3O_4 particles synthesized by using different volume ratios of ethylene glycol to diethylene glycol. (a) 20/0, 300 nm; (b) 10/10, 165 nm; (c) 5/15, 90 nm; and (d) 1/19, 18 nm (reproduced with permission from reference 34).

Fe are sensitive to the oxygen, it is necessary to surface-modify SPIOs or coat them with a layer of inert materials to protect them against oxidation and erosion. In addition, surface modification enables SPIOs to be multi-functional nanoparticles. Moreover, many functional groups such as $-\text{COOH}$, $-\text{NH}_2$ can be modified onto the surface of SPIO, so that the proteins, DNA, peptides, drugs can be linked to SPIOs and then actively be targeted to the selected tissues.

Surfactants or polymers are the most commonly used materials to modify SPIOs via the *in situ* and post-treatment method. The SPIOs synthesized by the co-precipitation are likely to agglomerate at physiological pH. To solve this problem, various materials such as PVA, Polyvinylpyrrolidone (PVP), tetramethylammonium hydroxide, citrate acid, phosphonate organic derivatives are added during the preparation, thus to be adsorbed on the surface of the SPIO to form a modified layer [43–46]. Actually, almost all high quality SPIO nanocrystals synthesized by the thermal decomposition are not water dispersible, which constricts their applications in the biology. Ligand exchange is an effective method to transform hydrophobic SPIO to be hydrophilic by replacing the hydrophobic surfactants with small molecules containing polar groups on the ends [47].

Recently, by using short-chain hydrophilic polyelectrolyte molecule polyacrylic acid (PAA) as the replacing ligand, Zhang *et al.* developed a refluxing method to conduct the ligand exchanging process in the polar diethylene glycol (DEG) solvent [48]. After the treatment, the PAA molecules bind to SPIO surface in the place of oleic acid and the resulted aqueous dispersion of the SPIO nanocrystals remains stable. Moreover, the hydrophobic SPIO nanocrystals can also be well dispersed into aqueous solution by assembling them to big hydrophilic nanospheres. Bai *et al.* used the microemulsion oil droplets as the confined templates within which the SPIO nanocrystals are assembled to spherical nanostructure after the

evaporation of the oil solvents [49]. The alkane chains of the surfactants locate on the outside surface of the nanospheres and the hydrophilic ends towards the solution, thus the as-obtained SPIO nanospheres can be well dispersed into water solution. Based on the similar method, supercrystalline SPIO colloidal spheres with tunable size have been achieved by utilizing the water dispersible SPIO nanocrystal micelles as precursors [50].

Coating SPIO nanocrystals with a protecting layer to form a core shell nanostructure is another effective method. Various inorganic and organic materials have been proved to be suitable coating precursors. Im *et al.* reported a facile Stöber method to synthesize SiO_2 coated SPIO nanospheres (SPIO@SiO_2) [51]. In this method, the size of SPIO@SiO_2 can be controlled by varying the concentrations of SPIO and Tetraethylorthosilicate (TEOS) precursor. Recently, Ge *et al.* developed a similar method for the preparation of monodispersed SPIO@SiO_2 microspheres [52]. Interestingly, these microspheres can be well dispersed in several solvents and assemble to photonic structures under the application of an external magnetic field. In addition, another layer of polystyrene can further be coated on the surface of the SPIO@SiO_2 to form a novel anisotropic nanostructure, in which the magnetic core is eccentrically located within the polystyrene shell [53]. In addition to protection, the coating layer can also endow SPIOs with other functions. By simply reducing HAuCl_4 in a chloroform solution of oleylamine, a uniform layer of Au shell can be coated on the surface of the SPIO nanocrystal at room temperature [54]. These nanoparticles can be used as the seeds for the preparation of the SPIO/Au/Au and SPIO/Au/Ag , where the shell thickness can be controlled by varying the concentration of the precursor. Most importantly, the additional coating changes the plasmonic properties of the final three-layer composite, in which the Au layer leads to a red-shift of the absorption peak and the Ag coating results in a blue-shift. Conductive polyaniline can also be successfully coated on the SPIO micro-

spheres to form well defined black-berry like nanostructures by an *in situ* polymerization in the presence of PVP surfactant [55]. With increasing of the concentration of the aniline, the shell thickness increases. The PVP molecules can not only stabilize the as-formed polyaniline but can also increase the compatibility between polyaniline and SPIO spheres. Further investigation indicates that polyaniline can directly be coated onto negatively charged SPIOs. During the preparation, the aniline may be reacted with the carboxylic acid groups (on the surface of SPIO) to give the $-\text{COO}-\text{H}_3\text{N}^-$ ion pairs, thus the aniline favors to polymerize on the surface of the SPIO nanospheres [56]. Similarly, other kinds of polymers such as the polystyrene, polymethylmethacrylate, polypyrrole, and phenol-formaldehyde can also be used [57-60].

Most of the above-mentioned methods are based on two steps synthesis, one is the preparation of the core and the other one is to coat a shell. To simplify the process, one-step method for the core/shell like magnetic nanostructures has drawn much attention. It was reported that the Au@Carbon and Ag@Carbon core shell nanostructure can be prepared by heating the aqueous glucose solution with relative precious metal ions [61]. Inspired by this work, carbon encapsulated SPIO nanocomposites were successfully achieved by an *in situ* reduction-carbonization hydrothermal method, in which the FeCl_3 and glucose were used as the starting materials [62]. Carbon is proved to be a more stable shell to resist the acid, base, and oxidation, in comparison to the traditional polymer or silica shells. Wang *et al.* showed that ferrocene can be used directly as the single reactant to produce the SPIO@Carbon core shell nanoparticles [63]. Under the application of a magnetic field, the suspension of the composite particles can diffract visible light which indicates their capability to form photonic crystal like microstructure. This phenomenon can also be found after storing the suspension for eight months and this result shows the as-prepared SPIO@Carbon exhibiting a high stability due to the presence of the carbon shells.

To further broaden the impact of SPIOs in diagnostic and therapeutic applications, many functional molecules are directly linked onto the surface of SPIOs. Xie *et al.* reported that the coating of dopamine and COOH-terminated polyethylene glycol on SPIO can improve their stability [64]. The size of the as-formed nanoparticles can be controlled by varying the length of the PEG molecules and these nanoparticles are stable in the cell culture media against the macrophage cell uptake. Furthermore, they found that chromone can be stored into the above modified SPIO nanoparticles and could be released via pH controlling [65]. Xu *et al.* developed a facile method to synthesize the nitrilotriacetic acid modified magnetic nanoparticles [66]. In this method, after immobilizing the Ni^{2+} ions, the above magnetic nanoparticles can selectively bind to hisidine-tagged proteins which enable it to be an effective method for protein separation and drug delivery. To our knowledge, the modification of the SPIO nanoparticles with $-\text{NH}_2$ functional groups by hydrolysis of 3-Aminopropyltriethoxysilane is the most facile method. During the synthesis, SPIO is firstly dispersed into the ethanol/ H_2O solutions, pH value is tuned by ammonia or NaOH, after introducing 3-Aminopropyltriethoxysilane, the mixture is refluxed, then the $-\text{NH}_2$ functional SPIO is prepared.

4. SPIO NANOPARTICLES CHARACTERISTICS AND CELL LABELING EFFICIENCY

Efficient capture of SPIOs, *in vitro* or *in vivo*, by target cells is essential for many of their biomedical applications. It is essential for cellular imaging, and cellular internalization of drug/SPIO composite is advantageous for therapeutic application when SPIO is used as a drug carrier. However, despite the large number of cell labeling studies that have been performed with SPIOs of differing size and surface charge, it still remains unclear which SPIO configuration provides optimal affinity for non-phagocytic cells. Ferumoxides (Feridex[®] IV, Berlex Laboratories; and Endorem[®], Guer-

bet) possess a dextran coating, while Ferucarbotran (Resovist[®], Bayer Healthcare) has a carboxydextran coating [2-4]. Ferumoxides are an SPIO colloid with a hydrodynamic particle size of 120-180 nm, while Ferucarbotran is an SPIO colloid with a hydrodynamic particle size ranging between 45 and 60 nm. However, there is a lack of efficient binding of dextran coated nanoparticles on the plasma membrane, which limits the capability of cell internalization to the fluid phase endocytosis pathway [67-69].

The cellular uptake and more generally their biological behaviors depend on several physicochemical parameters of SPIOs including their size, shape, polydispersity, charge and structure of the coating [17]. When taking into account the coating, "large" (> 50 nm of hydrodynamic diameter) SPIOs, such as Ferumoxides or Ferucarbotrans show a greater uptake than smaller SPIOs, i.e. Ferumoxtran-10 (Sinerem[®], SPIO with hydrodynamic size of 15-30 nm and dextran coating, Guerbet) and SHU-555C (SPIO with hydrodynamic size of 21nm and carboxydextran coating, Bayer Healthcare) respectively, as shown on the human promonocytic cell line THP-1 [70]. The *in-vitro* uptake of Ferumoxides by mouse peritoneal macrophages was found to be dose-dependently inhibited by polyinosinic acid and fucoidan, thus suggesting the involvement of a scavenger receptor A-mediated endocytosis for this nanoparticle [71]. The positively charged collagen-like domain of the scavenger receptor may participate in the recognition of dextran-coated SPIOs. Uptake of Ferumoxides through scavenger receptors was confirmed by Chao *et al.*, who demonstrated that the carbohydrate receptor pathway (mannose receptor CD206) is not involved in this phenomenon [72].

Different strategies have been employed to improve the efficiency of magnetic labeling of a wide variety of cells. First strategy is to substitute the fluid phase endocytosis pathway of SPIOs with the more efficient receptor mediated endocytosis pathway by coupling SPIO particles with specific ligands. Some authors exploited the ubiquitous transferrin receptor to shuttle transferrin-coupled dextran coated nanoparticles into cancerous cells as well as into neural progenitor cells [73-75]. The cell capture of transferrin-coupled nanoparticles was two to four times higher compared to that of the dextran-coated particles and was dependent upon the level of cell expression of the transferrin receptors. Some authors [76-77] performed a graft on a cross-linked dextran coated superparamagnetic nanoparticles with a membrane translocating signal peptide HIV-1 Tat protein which is known to freely travel through cellular and nucleic membranes, and succeeded in improving the magnetic labeling efficiency. Compared to dextran coated nanoparticles, the uptake was enhanced by two to three orders of magnitude in hematopoietic CD34+ cells, mouse neural progenitor cells, human CD4+ lymphocytes or mouse splenocytes, attaining 10 to 30 pg of iron per cell [77-78]. During *in vitro* cellular labeling procedures, some authors use transfection agents to increase SPIOs cell labeling efficiency [79]. Transfection agents are highly charged macromolecules that have been used to transfect oligonucleotides into cells via electrostatic interaction, which results in endosome formation. Transfection agents are toxic to cells, and their toxicity is proportional to the transfection agent concentration [80]. It is advantageous if a high intracellular labeling efficiency can be achieved without the use of any transfection agent.

Surface charge is an important factor for intracellular delivery of exogenous materials. It was found that ionic carboxydextran-coated Ferucarbotran performed better than non-ionic dextran coated Ferumoxides for cell labeling [81]. Cationic surfaces of exogenous material have been shown to facilitate cellular internalization [82-83]. For the cellular uptake of SPIOs in non-phagocytic T cells, it was reported that the aminated surfaces of SPIO particles provide an inherent surface charge, facilitating cellular interaction [84]. In a recent study, we systematically compared cancerous cell lines MCF-7, MDA-MB-231, HT-29, HepG2, PC-3 and U-87 MG, as well as mouse bone marrow derived mesenchymal stem cells

(MSCs), mouse macrophage cells (RAW 264.7) and mouse fibroblast cells (L929) with aminosilane ($\text{SiO}_2\text{-NH}_2$), SiO_2 or dextran coated SPIO as well as bare SPIO nanoparticles (SPIO core size: 7 nm; overall size: ~ 15 nm) [85]. We demonstrated that cellular uptake efficiency of SPIO nanoparticles was dependent on the characteristics of cell lines as well as the surface coating of nanoparticles. Among these two factors, the biological nature of cell line may have the prior importance. MCF-7, MDA-MB-231, and HT-29 cells had poor uptake efficiencies for all four types of SPIO nanoparticles. On the other hand, L929, RAW 264.7, HepG2, PC-3, U-87 MG cells, and MSCs displayed substantial nanoparticle cellular uptake capabilities. It was also observed that all these six mammalian cell lines showed the highest cellular uptake for SPIO@ $\text{SiO}_2\text{-NH}_2$ nanoparticles (Fig. 2). Our study may also suggest that cancers with biological features similar to breast cancer cells MCF-7, MDA-MB-231 and colon cancer HT-29 cells may be less amenable to certain types of targeted therapy, while cancers with biological features similar to cancerous cells HepG2, PC-3 and U-87 MG may be more responsive to nanoparticle assisted targeted therapies. We have previously reported that surface amine modification enhances labeling efficiency for rabbit MSCs of SPIO@ $\text{SiO}_2\text{-NH}_2$ nanoparticles by 4-fold compared to SPIO@ SiO_2 nanoparticles (Fig. 3) [86-87]. That finding agreed well with the current result of mouse MSCs (Fig. 2F). In another study, the high cellular labeling efficiency of SPIO@ $\text{SiO}_2\text{-NH}_2$ nanoparticles was also observed in human osteosarcoma line U2OS [88].

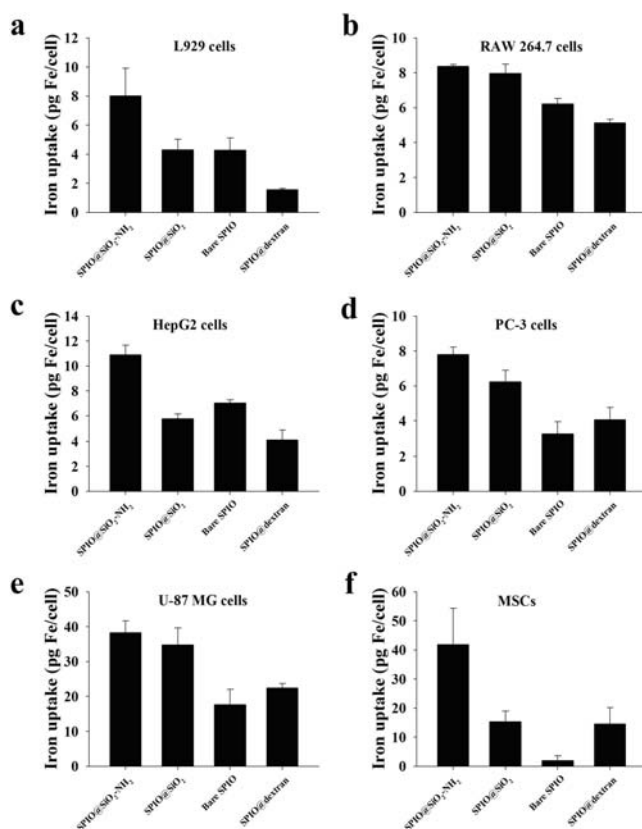


Fig. (2). Intracellular iron content in L929, RAW 264.7, HepG2, PC-3, U-87 MG, and primary cultured mouse MSCs after 24 hours incubation of SPIO nanoparticles with iron concentration at $4.5 \mu\text{g/mL}$. Note: Data were expressed as means \pm standard deviations from three experiments. Abbreviations: MSC, mesenchymal stem cell; SPIO@ $\text{SiO}_2\text{-NH}_2$, aminosilane-coated SPIO nanoparticles; SPIO@ SiO_2 , SiO_2 -coated SPIO nanoparticles; SPIO@dextran, dextran-coated SPIO nanoparticles (reproduced with permission from reference 85).

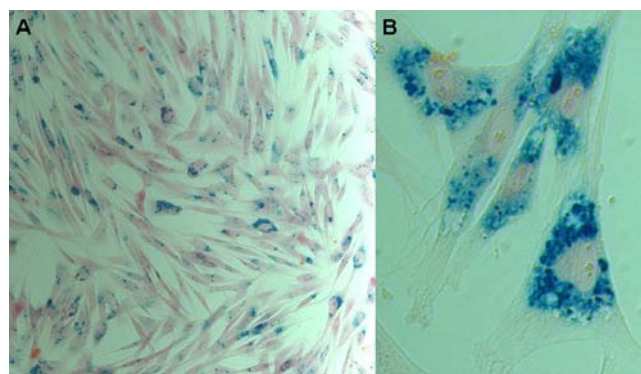


Fig. (3). Optical microscopy images of the rabbit MSCs with Prussian blue staining, demonstrating the SPIO@ $\text{SiO}_2\text{-NH}_2$ nanoparticle distribution within mesenchymal stem cells (original magnification: $200\times$). **A)** Image showing close to 100% labeling efficiency. **B)** Image showing numerous SPIO nanoparticles in four MSCs (reproduced with permission from reference 86).

Under pH value less than 8, the protonation of amino groups on aminosilane-modified magnetic nanoparticles occurs, resulting in surface positive charges [89] and SPIO@ $\text{SiO}_2\text{-NH}_2$ nanoparticles are positively charged. It is also known that plasma membranes possess large negatively charged domains, which repel anionic nanoparticles, and cationic surfaces can facilitate cellular internalization [84]. Due to the hydroxyl group present on the surface of SPIO@ SiO_2 and bare nanoparticles, these two nanoparticles are negatively charged [90]. This may partially explain why SPIO@ $\text{SiO}_2\text{-NH}_2$ nanoparticles possess higher cellular labeling efficiency than SPIO@ SiO_2 nanoparticles. Osaka *et al.* also reported a correlation between the surface charge of SPIOs and their cellular uptake efficiency into different cell lines [69]. SPIOs with a positive charge showed higher internalization into human breast cancer cells compared to negatively charged SPIOs; whereas there was no difference in the degree of internalization into human umbilical vein endothelial cells. In our study [85], compared to SPIO@ $\text{SiO}_2\text{-NH}_2$ or SPIO@ SiO_2 nanoparticles, non-coated and dextran coated SPIO nanoparticles were found to be less uptaken in all six cell lines. Kunzmann *et al.* reported that silica-coated SPIO nanoparticles were taken up to a greater extent when compared to dextran-coated particles in primary human macrophages [91].

On the other hand, Wilhelm *et al.* presented a class of SPIOs bearing negative surface charges [67]. These anionic nanoparticles show a high affinity for the cell membrane and, as a consequence, are captured by HeLa cells with an efficiency three orders of magnitude higher than the dextran-coated iron oxide nanoparticles. It was noted that surface coating of anionic particle with albumin strongly reduces the nonspecific interactions with the plasma membrane as well as the overall cell uptake. Previous studies reported cellular uptake of dextran coated nanoparticles varying from 0.011 to 0.118 pg of iron per cells (1 h incubation at 37°C ; $[\text{Fe}] = 2\text{mM}$) in different tumor cells and a maximum load of 0.97 pg in primary isolated peritoneal mouse macrophages. In contrast, saturating uptake of anionic nanoparticles was found to be up to 40 pg per cell in HeLa cells for $[\text{Fe}] = 15\text{mM}$ and up to 10 pg per cell in macrophages for $[\text{Fe}] = 1.5\text{mM}$ [67].

Ferumoxides and Ferucarbotran both have negative surface charge. Cellular labeling with SPIOs such as Ferumoxides and Ferucarbotran occurred randomly because of an absence of driving force, thereby showing irregular engulfment efficacy. Recently, heparin-coated SPIO (HSPIO) has been developed due to specific function of heparin molecule [92-94]. Heparin, with a molecular weight between 3 to 30 kDa, is composed of sulfated glycosamino-

glycan and is widely used as an anticoagulant medication. When treated with the HSPIOs, stem cells are able to engulf ~4-fold larger amount of HSPIOs into cytosol when compared to Ferumoxides treatment [92]. For the labeling of stem cells, Ferumoxides were treated with stem cells with long treatment time (~24 h) and high concentration, and the amount of the engulfed iron had wide range (1.47 - 17.9 pg Fe/cell) [95]. On the other hand, HSPIOs can easily enter stem cells, though exposed to stem cells for 1 h incubation. Other previous studies also demonstrated that hydrophilic heparin coated onto the surface of biomaterials could facilitate cell adhesion to the cell membrane surface due to the enhanced hydrophilicity [96-98].

Low-intensity pulsed ultrasound (LIPUS) has been used to facilitate the uptake of SPIOs by cells that do not express high endocytosis capacity. In an example of the human osteosarcoma cell line U2OS, it was reported that LIPUS with the same parameters as those used in clinical application to accelerate bone fracture healing (1.5 MHz, duty cycle 1:4, spatial-average temporal-average intensity 30 mW/cm²) was able to facilitate the uptake of small SPIOs (overall diameter 8 nm) by U2OS cells in an exposure duration dependent manner [88].

Surface coating can influence nanoparticles cellular uptake behavior as well as their cytotoxicity. In the study of cellular uptake of SPIOs in non-phagocytic T cells, Thorek & Tsourkas found that there was no trend correlating increased or decreased SPIOs particle size with labeling efficiency [84]. However, they found that highly-aminated SPIOs with a diameter of 107 nm had a high cell labeling efficiency. Thorek & Tsourkas also suggested that despite their high R2 values and large iron contents, SPIO particles greater than 200 nm had limited applicability in labeling non-phagocytic cells. With T cell, it was reported that negligible to low levels of cell death were observed for SPIO particles of a number of diameters incubated at concentrations of 10 and 50 µgFe/mL, respectively, except for the surface aminated 107 nm SPIO which exhibited some cell death even at 10 µg/mL and this effect was exacerbated at increased concentrations [84]. However, when the amines on the 107 nm particle were completely blocked, cell death was reduced to negligible levels; meanwhile, cell internalization was also reduced extensively. These results show that the high driving force for cell internalization imparted by the positive charge due to aminated surface on SPIOs can lead to T cell death. In our study, the dependence of cytotoxicity on surface coating of SPIO nanoparticles was investigated using the mouse macrophage RAW 264.7 cells. Our results showed that the SiO₂ coated SPIOs with amine surface modification and bare SPIO and dextran coated SPIO nanoparticles (all approximately 10nm) did not affect the cell viability of RAW 264.7 cells, even at an iron concentration of 200 µg/ml [85]. However, SiO₂ coated SPIO nanoparticles (approximately 10nm) negatively affected RAW 264.7 cell viability at iron concentrations from 10 to 200 µg/ml in a dose-dependent manner [85]. Gozal *et al.* reported that RAW 264.7 cells are sensitive to silica, and exhibit enhanced TNF-α production and NF-κB activation which lead to cell apoptosis [99]. This result is also consistent with the finding reported by Kunzmann *et al.* that small silica coated SPIO nanoparticles (30 nm and 50 nm) rather than dextran-coated nanoparticles displayed dose-dependent cytotoxic effect [91]. The aminosilane improves the biocompatibility of silica coating which may be partly due to the organic modification of the silica coating and limits the interaction between silica and intracellular organelles.

Micrometer-sized iron oxide particles (MPIO) uptake in non-phagocytic cells has been accomplished, but is limited by the additional conjugation work and cost of using an antibody mediated approach [100], which must be species specific and may induce adverse cellular events. Large particles, over 200 nm in diameter, possess much greater amounts of iron per particle, and thus theoretically require few or single particles per cell to be used. However, during *in-vitro* process, these particles suffer from gravita-

tional sedimentation, decreased efficiency of cell labeling, and in some cases, free particles are incompletely removed from labeled cells. This may not be a problem with adherent and/or phagocytic cell systems, but significantly hampers their efficacy as magnetic labeling probes for non-phagocytic suspended cells [84].

5. SPIO NANOPARTICLES FOR MAGNETIC RESONANCE IMAGING CONTRAST

MRI contrast agents have made a significant impact in the use of MRI for various clinical indications. Since the introduction of the first MRI contrast agent Gd-DTPA (Magnevist[®], Bayer Healthcare) in 1988, there has been a tremendous increase in the number of contrast-enhanced MRI examinations. MRI contrast agents contain paramagnetic or superparamagnetic metal ions that affect the MRI signal properties of surrounding tissue. A conglomerate of numerous nano-sized iron oxide crystals coated with dextran or carboxy-dextran forms SPIO contrast agents [2-4]. Two SPIO particle formulations have been approved by the regulatory bodies, namely Ferumoxides (Feridex[®] IV, Berlex Laboratories; and Endorem[®], Guerbet) and Ferucarbotran (Resovist[®], Bayer Healthcare). Ferumoxides and Ferucarbotran were both approved specifically for MR imaging of the liver. However, radiologists are now using other new tools for liver imaging, only Resovist[®] is still marketed in Japan. After intravenous administration, due to their size Ferumoxides and Ferucarbotran particles are cleared from the blood by phagocytosis accomplished by reticuloendothelial system (RES) so that uptake is observed in the normal liver, spleen, bone marrow, and lymph nodes. After the intracellular uptake, SPIOs appear in the lysosomes, and turn into a soluble, nonsuperparamagnetic form of iron that becomes part of the normal iron pool (eg, ferritin, hemoglobin) [101]. Phagocytosed SPIO particles in Kupffer cells in the liver produce strong T2/T2* relaxation effects in normal hepatic parenchyma. Following the administration of this agent, because of a homogeneous distribution of reticuloendothelial cells in the healthy liver parenchyma, the liver negatively enhances on T2- or T2*-weighted images (ie, it turns dark), resulting in increased conspicuity of pathologic lesions that do not contain reticuloendothelial cells (Fig. 4). The degree of SPIO uptake and the consecutive extent of signal intensity drop are used to differentiate and characterize lesions [4].

The detection of liver metastatic lesions is improved with SPIO agent, as well as cholangiocellular carcinoma, due to the absence of Kupffer cells within these lesions. Undifferentiated hepatocellular carcinoma (HCC) usually demonstrates no change in signal intensity when compared with T2/T2*-weighted images in unenhanced and SPIO-enhanced imaging. This leads to an improvement in the contrast-to-noise ratio of the lesion with subsequent improvement of demarcation as well as visualization and an increased detection rate for HCC. On the other hand, lesions containing reticuloendothelial cells, such as focal nodular hyperplasia, may become isointense to normal liver because of a decreased lesion-to-liver contrast ratio [103]. Phagocytic activity might overlap among some borderline lesions. One study found no significant difference in number of Kupffer cells between well-differentiated HCC and surrounding liver tissue [104]. Double-contrast MR imaging of SPIO- and Gd-dynamic MR imaging have also been used to assess liver fibrosis [105]. Overall the uptake of SPIO based agents in clinical practice has been much less than expected.

Ferumoxtran-10 (AMI-227; Combidex[®], AMAG Pharma; Sinerem[®], Guerbet) has a small size and hydrophilic coating resulting in a longer blood half-life. These particles are subsequently phagocytosed by macrophages and accumulate in the lymphatic system or inflammatory foci. Normal lymph nodes are characterized by a dramatic signal drop on T2*-weighted images, whereas malignant lymph nodes, being devoid of macrophages, do not accumulate iron oxide particles and maintain a high MRI signal inten-

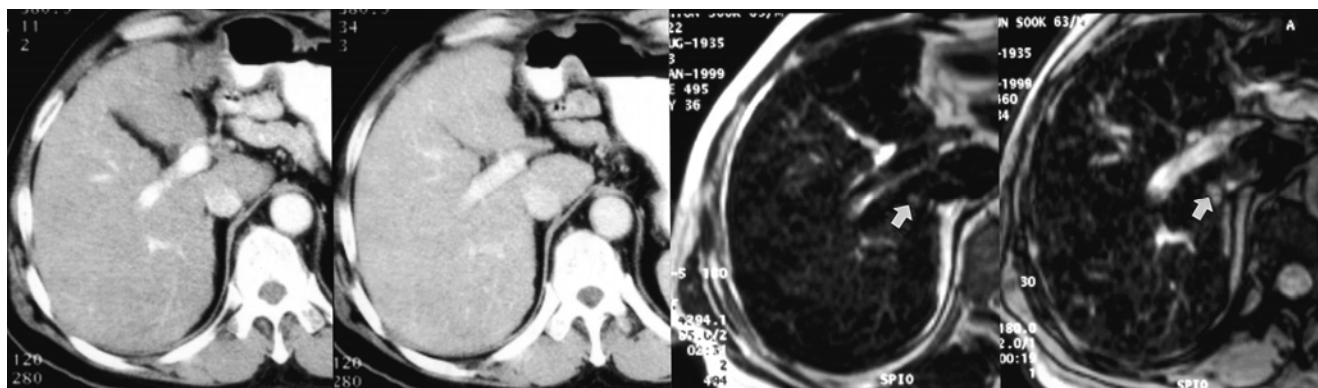


Fig. (4). One 0.8-cm hepatocellular carcinoma was found in the liver of a 63-year-old man. **A.** Neither the arterial-phase CT image (left) nor the portal venous-phase CT image (right) reveals the presence of a lesion. **B.** SPIO-enhanced respiratory-triggered T2-weighted turbo spin-echo image (left) and breath-hold T2*-weighted fast image obtained with steady state precession (right) depict the tumor as an area of high signal intensity (arrows). The tumor was surgically confirmed (reproduced with permission from reference 102).

sity (Fig. 5). The development of this product has recently been halted in Europe as well as in the US.

The therapeutic use of stem and progenitor cells as a substitute for malfunctioning endogenous cell populations has received considerable attention. The development and evaluation of stem cell-based therapies desire a qualitative and quantitative assessment of their distribution to target organs and their engraftment. To be visualized with MRI, before *in vivo* administration, these stem cells can be *in-vitro* labeled with SPIOs. MRI tracking of the stem cells will then depend on magnetic particle labeling efficiency and a low body clearance rate. Prussian blue staining has commonly been used to confirm that the stem cells are labeled with SPIO particles *in vitro*. However, it is not easy using Prussian blue stain to confirm whether SPIO particles are labeled intracellularly or whether they are merely attached to the surface of cells. It can be assumed that the SPIO particles that are merely attached to the stem cells surfaces are more likely to fall off the cells during *in-vitro* handling in the later stages and also after being transplanted into the *in-vivo* system. This leads to the possibility that stem cells that initially appeared to have been properly labeled based on Prussian blue staining evidence become “unlabelled” later on [106-107]. The fate of intracellularly labeled SPIO particles is not yet fully understood. Some SPIO particles will eventually be biodegraded within the cells after a period of time. Therefore, not all the stem cells labeled with SPIO particles *in-vitro* will have the presumed level of SPIO particles or a sufficient amount of such particles to render the stem cells trackable *in-vivo* by MRI after transplantation. Some SPIO labeled stem cells may actually die after being transplanted into the *in-vivo* system. Although these dead stem cells can be visualized with MRI, they no longer have biological functions. Dead stem cells and their debris will be engulfed by macrophages or other cells with a similar function, such as glial cells in the brain and spinal cord. The SPIO particles removed from stem cells via exocytosis and those that dropped off from the surface of the stem cells are also likely to be taken up by monocytes/macrophages, especially when stem cells are delivered intravascularly; SPIO particles will also be deposited in lymph nodes. In this case, MRI will also visualize these monocytes/ macrophages and lymph nodes [107]. In addition, MRI is an insensitive technique, despite *in-vitro* optimized scenario single cell detection has been achieved in phagocytic cells with clinically approved SPIOs [108-109], the *in-vivo* detection limit is likely to be around 1,000 stem cells. In addition, SPIO stem cell labeling is not an FDA approved indication till now, how SPIOs affect the function and fate of stem cells requires further clarification. Despite initial reports that labeling of stem cells with SPIO is safe without affecting stem cell viability, recent studies

suggested that SPIO-labeling may affect the metabolism and some functions of stem cells [110-111]. On the other hand, though how SPIO cell labeling will be used clinically remains unclear, *in-vivo* animal study with this technique does provide a useful tool to understand the mechanism of how stem cells will function to repair the damaged tissues [112]. The value of SPIO-based imaging for the follow up of *in-vivo* pharmacodynamics effects of the angiotensin II receptor antagonist irbesartan has been evidenced in ApoE^{-/-} mice 48 hours after the administration of SPIOs [113]. The rapidly evolving field of small animal imaging that allows non-invasive and real-time evaluation of the natural history of disease, or efficacy of treatments as well as the wide availability of high-resolution imaging equipment is crucial in translational research.

As noted previously, following intravenous injection, SPIO is incorporated into macrophages via endocytosis. The uptake of SPIOs by phagocytic monocytes and macrophages provides a valuable *in-vivo* tool by which MRI can be used to monitor the involvement of macrophages in inflammatory processes, such as multiple sclerosis, traumatic nerve injury, stroke, brain tumors, and vulnerable plaque in carotid artery [114]. Capture of SPIOs by inflammatory lesions results in hypersignal on T2/T2*-weighted MR sequences. This important issue can be potentially integrated in daily clinical practice of radiologists. Most of the clinical studies involving SPIOs with “stealth behavior”, i.e. escaping to the reticuloendothelial system during early phases following injection to reach “deep” inflammatory foci, were performed with Ferumoxtran-10. Saleh *et al.* [115] performed an MRI study with Ferumoxtran-10 in ischaemic stroke patients and observed macrophage activity in all patients. For multiple sclerosis, Dousset *et al.* used Ferumoxtran-10 particles to demonstrate the visualization of macrophage activity in patients with relapsing-remitting multiple sclerosis [116]. Neuwelt *et al.* conducted clinical studies with MRI monitoring of macrophages in brain tumors [117]. The macrophage MRI detection with SPIOs of tumor morphology might facilitate the surgical resection or biopsy of brain tumors. Of note, positive signal enhancement can also be observed in the case of low local concentration of SPIOs in the tissue.

Several clinical studies have shown that the dextran-coated ferumoxtran-10 targets macrophages located in atherosclerotic aorta and pelvic arteries or in stenotic carotid arteries [118-120]. Trivedi *et al.* reported that, 24-36 h after infusion, Ferumoxtran-10 particles accumulated in macrophages of carotid atheroma which was detectable *in-vivo* by MRI [121]. The ATHEROMA (Atorvastatin Therapy: Effects on Reduction of Macrophage Activity) study investigated the effects of low- and high-dose atorvastatin on carotid plaque inflammation as determined by ferumoxtran-10 enhanced

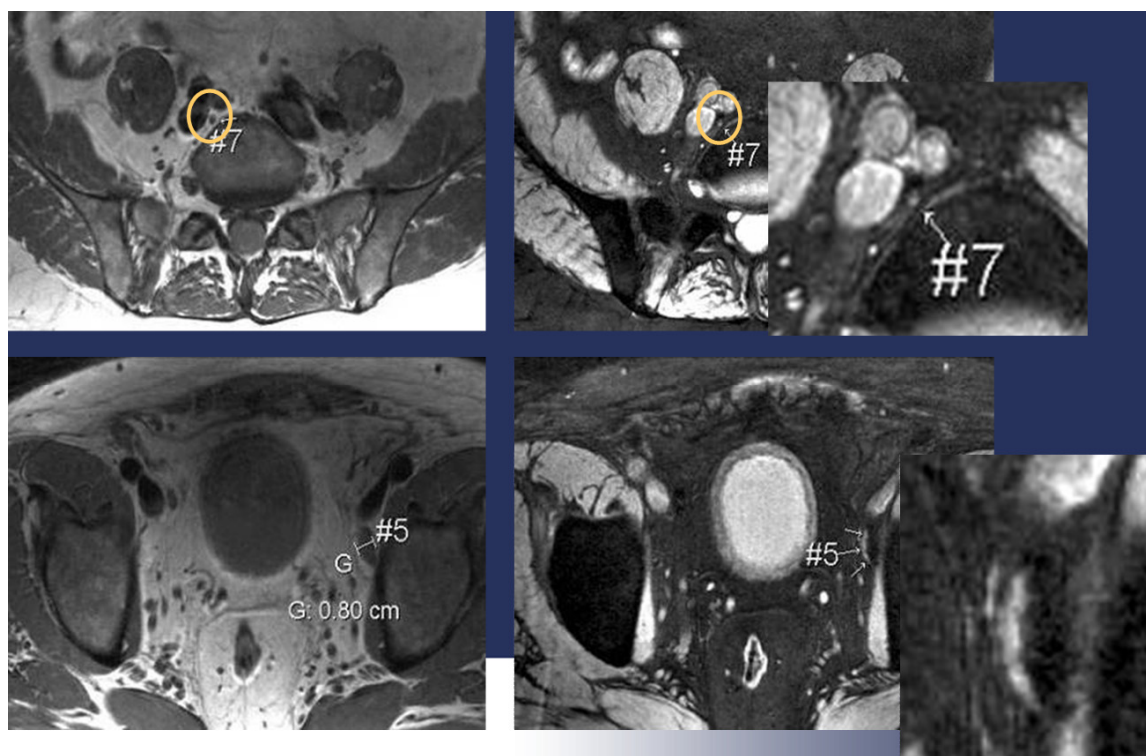


Fig. (5). This figure shows that how small lymph nodes supposed to be benign due to their size can be malignant. Images on the left hand are pre-contrast images, while the post-contrast images on the right show hypersignal intensity small lymph nodes, which is a sign of malignancies. MRI at 3T allows a perfect depiction of these small lesions with high spatial resolution (Courtesy of Prof. Dr. Jelle Barentsz, Prostate MR-Center of Excellence, Afdeling Radiologie, Radboud Universiteit Nijmegen Medisch Centrum, the Netherlands).

carotid MRI in 47 patients with carotid artery stenosis > 40%. This trial showed the evidence that aggressive lipid-lowering therapy with high-dose of atorvastatin over a 3-month period is associated with significant reduction in SPIO-defined carotid plaque inflammatory foci [122]. This was the first prospective clinical study that intended to correlate the *in-vivo* effects of statin therapy on carotid plaque inflammation. The exposure period of atheromatous plaque to circulating SPIOs is critical for the uptake of SPIOs. In hyperlipidemic rabbits, the *in vivo* MRI enhancement was found to be higher with the long half-life agent ferumoxtran-10 as compared to that obtained with ferumoxytol, another SPIO of similar size with shorter half-life, whereas *in vitro* macrophage phagocytosis was greater with ferumoxytol [123]. The reproducibility and repeatability of vascular inflammation imaging using SPIO need to be assessed in comparison to that of 18 F-fluorodeoxyglucose (FDG) positron emission tomography (PET) associated with computed tomography (CT). Furthermore, because of the proximity of the lymphatics to the arterial wall and the capture of SPIOs by lymph nodes, an interfering blooming effect might be observed [124]. The issue of quantification of SPIO-based carotid plaque $T2^*$ weighted imaging has also been questioned [124]. However, recent clinical data suggest that quantitative $T2^*$ measurement is feasible [125]. Therefore, SPIO based cellular MRI provides an imaging biomarker looking into the diverse physiopathological phenomena in clinical scenario.

Furthermore, coupling of a “pharmacophore” (such as antibodies, fragments of antibodies, peptides, small organic ligands) is a common approach to target overexpressed receptors (HER2/neu, EGFR, etc.), integrins, vascular cell adhesion molecule 1 (VCAM-1), etc. and thus allows transition from cellular imaging (with unfunctionalized SPIOs or “contrastophores”) to molecular imaging [3]. *In vitro* and *in vivo* preclinical proofs of this concept are available for several such nano-objects. However, the intrinsically low sensitivity of MRI limits the selection of molecular targets of clinical

interest [17]. The non-specific lesion enhancement associated to diffusion of vectorized nanoparticles must be distinguished from specific enhancement induced by binding and internalization onto cells overexpressing the target of interest. Therefore, relevant control groups are mandatory in preclinical studies to evidence the specificity.

SPIOs with prolonged blood half-life may be used as blood pool agents, using a T1 sequence for MR angiography [126], microvascular permeability and tumor blood volume, where signal enhancement reflects the regional blood volume [3]. Using $T2/T2^*$ sequences and provided they have a prolonged blood half-life, intravenous bolus administration of these nanoparticles can allow measurements of steady-state cerebral blood volume (CBVss) and microvessel size index measurements [3]. In addition to its interest as a research tool for physiological studies [127], SPIO-based functional imaging may be of clinical value, for example for the non-invasive localization of eloquent cortex before neurosurgery. CBVss-based functional imaging has a higher sensitivity compared with BOLD imaging as well as a better spatial resolution [128]. SPIO (monocrystalline iron oxide nanoparticles, MIONs) was found in awake macaque monkeys to increase functional sensitivity at 3 Tesla MRI by an average factor of 3 across the brain for a stimulus of long duration [129]. Functional imaging can be a helpful tool in both the preclinical and clinical steps of the development of a central nervous system drug candidate [130]. The current absence of marketing authorization of small SPIOs with long half-lives does not preclude their use for preclinical development studies.

6. SPIO NANOSTRUCTURE ASSISTED DRUG DELIVERY.

Various nanostructures are proposed as carrier for therapeutic drugs, particularly anticancer drugs. When administrated *in-vivo* intra-vascularly, nanoparticles preferentially accumulate at tumor

sites through enhanced permeability and retention (EPR) effect, as tumor-associated neovasculatures are highly permeable, allowing the leakage of circulating nanoparticles into the tumor interstitium, and also many tumors lack an effective lymphatic drainage, leading to subsequent nanoparticle accumulation [131]. In addition, drugs associated with nanoparticles may avoid recognition by the P-glycoprotein efflux pump which is the best known mechanism of drug resistance, leading to higher intracellular drug concentrations [132]. Though SPIO is not associated in this case, one successful nanotechnology based on paclitaxel formulation approved by the FDA is Abraxane™ (Abraxis, Celgene) for treating metastatic breast cancer. Abraxane is an albumin-paclitaxel nanoparticle formulation prepared by high-pressure homogenization of paclitaxel in the presence of serum albumin into a nanoparticle colloidal suspension with size range of 100–200 nm [133].

SPIOs have emerged as promising drug carriers. SPIOs are highly biocompatible, with the iron ion from the degradation enters the body iron pool. SPIOs employed in drug delivery include nanospheres, nanoshell, liposomes and microspheres. Drugs are bound to SPIO surface or encapsulated in magnetic liposomes and microspheres. If the drug is loaded on the surface of SPIOs, drug payload can quickly be released upon injection into the *in-vivo* environment (i.e. burst effect). In order to reduce the burst effect, SPIO has been prepared with a cross-linked poly (ethylene glycol)-co-fumarate (PEGF) coating. Tamoxifen was loaded onto the surface of coated SPIO (via hydrogel properties of PEGF), and the results showed that the cross-linked PEGF coating reduced the burst release by 21% in comparison with the non cross-linked tamoxifen loaded particles [134]. SPIOs with a mesoporous structure were also prepared via simple solvothermal method and doxorubicin was loaded, a favorable loading capacity and release kinetics were demonstrated [135]. In other approaches, phospholipid vesicles incorporating SPIOs (magnetic liposomes) were filled with drugs and used for targeted delivery applications [136-137]. Magnetic microspheres have been formed from encapsulation of SPIOs (with core size of 5–15 nm) in biocompatible, non-toxic (FDA approved) and biodegradable polymeric microspheres, such as PLGA and poly (L- or DL-lactide) (PLA) [9]. Since most of polymeric coatings in SPIOs are selected from hydrogel categories, the drug release from these hydrogel shells can be engineered by controlling their physical and chemical properties. Permeability, temperature sensitivity, pH sensitivity, osmolarity, sensitivity, charge, surface functionality, swelling, biodegradability, and surface biorecognition sites are major mechanisms for controlled drug release applications of hydrogels [138]. For instance, by using the thermal sensitivity of hydrogels on the surface of SPIO, the release of chemotherapeutic drugs can be controlled by local heating using an alternating current magnetic or electromagnetic field. Magnetoliposomes, which contain SPIOs of 8 nm diameter, can release the drug upon magnetic field irradiation [139]. Since the magnetoliposomal membrane has a phase transition temperature of 42 °C, the release of drug can be related to the local heating of the liposomal membrane.

More than 40% drug candidates identified by high-throughput screening are poorly water soluble [140]. These water insoluble drugs show decreased systemic bioavailability when orally administered or hamper the ability to be administered through the intravenous route. Porous or hollow structured materials have been considered for delivery of water-insoluble anticancer drugs. SPIO based hydrophobic drug carriers commonly comprise magnetic nanoparticulate cores with an organic (i.e. oleic acid) [141] or inorganic (i.e. mesoporous silica) shell [142], and the therapeutic agents are encapsulated within the shell structure. Recently, SPIO nanoshells have successfully been synthesized by Cheng *et al.* [143] and Iram *et al.* [144]. Hollow SPIO nanoshells have large fraction of volumes in their inner space, which can be used as a reservoir for storing hydrophobic drugs. With curcumin and doxorubicin base as model drugs, intracellular delivery of hydro-

phobic anticancer drugs by hollow structured SPIO nanoshells (hydrodynamic diameter: 191.9 ± 2.6 nm) was studied in gliomablastoma U-87 MG cells [145]. It was demonstrated that encapsulation by SPIO nanoshells enabled good aqueous dispersion of the hydrophobic drugs. In lysosome-mimicking buffers with a pH of 4.5–5.5, pH-dependent drug release was observed from curcumin and doxorubicin loaded SPIO nanoshells (curcumin/SPIO or doxorubicin/SPIO). After internalization by U-87 MG cells, SPIO nanoshells were localized at the acidic (pH ~4.5) compartments of endosomes and lysosomes (Fig. 6). Compared with free drug, the intracellular curcumin content delivered via curcumin/SPIO was 30 folds higher. Increased intracellular drug content for doxorubicin base delivered via doxorubicin/SPIO was also confirmed, together with a fast intracellular doxorubicin release attributed to its protonation in the acidic environment (Fig. 7). Doxorubicin/SPIOs enhanced caspase-3 activity by twofold compared with free doxorubicin base. The concentration inducing 50% cytotoxic effect (CC₅₀) was 0.05 ± 0.03 µg/ml for doxorubicin/SPIO, while it was 0.13 ± 0.02 µg/ml for free doxorubicin base [145].

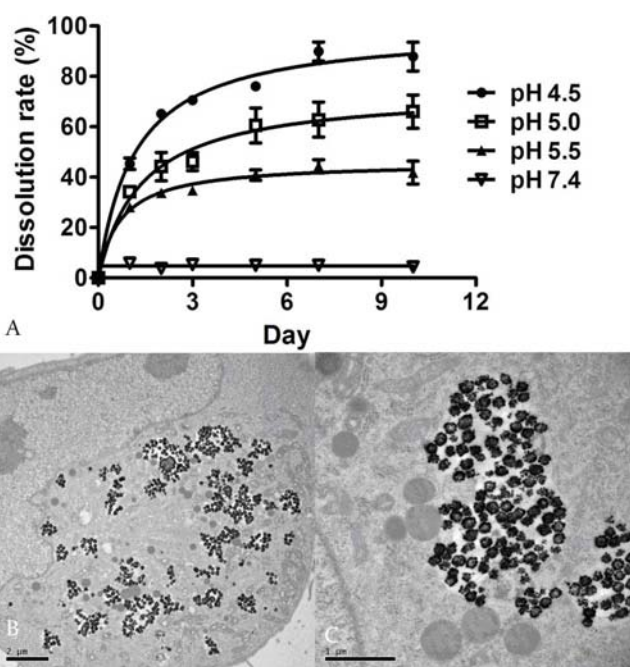


Fig. (6). A: pH-dependant SPIO nanoshell dissolution in endosomes/lysosomes mimicking acidic buffers. 50 µg/ml SPIO nanoshells were incubated with 20 mM citrate buffer at pH 4.5, 5.0, 5.5 or PBS at pH 7.4. The dissolution rate was calculated by measuring the iron concentration of the supernatants. B & C: TEM images of U-87 MG cells after incubation with 5 mg ml⁻¹ SPIO nanoshells for 24 h. Intracellular SPIO nanoshells are distributed in the endosomal/lysosomal compartments, but not in the nucleus and other supermicrostructures, and a fraction of nanoshells is disintegrated (reproduced from reference 145 with permission).

Compared with other nanoparticle drug carriers, one of the important advantages of drug attached/encapsulated SPIOs is that these composites can be delivered via magnetic targeting. In addition, the *in-vivo* distribution of these drug/SPIO composites can be monitored by MRI [146]. The first application of magnetic drug delivery systems was developed by Widder *et al.* [147]. In magnetic targeting, SPIOs loaded with anti-cancer agents are intravenously or intra-arterially administered. When applying an external high-gradient magnetic field at the desired site, for example solid tumor site, the drug/SPIO composites can be accumulated locally. In most cases, the magnetic field gradient is generated by a strong permanent magnet, fixed outside the body over the target site. When the

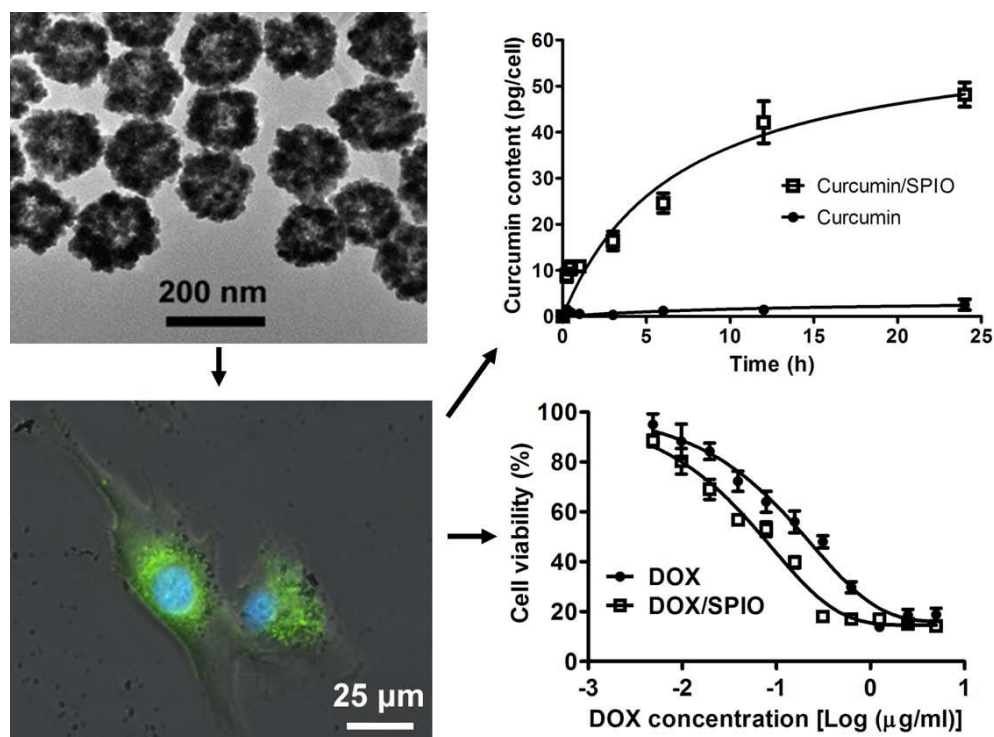


Fig. (7). U-87 MG cells were incubated with 5 $\mu\text{g/ml}$ SPIO nanoparticles for 24 h. Cells were subsequently stained with 1 μM LysoSensor™ Green DND-189 (green) and 100 ng/ml Hoechst 33342 (blue) for 30 min, and then observed by the fluorescent microscope. The merged images of phase contrast, LysoSensor green and Hoechst 33342 staining indicate the co-localization of endosomes/lysosomes and SPIO nanoshells. Scale bar = 25 μm . Intracellular delivery of hydrophobic anticancer drugs by hollow structured SPIO facilitated intracellular curcumin delivery and also enhanced cytotoxic effect for doxorubicin (DOX) (reproduced from reference 145 with permission). (The color version of the figure is available in the electronic copy of the article).

magnetic forces exceed the linear blood flow rates in arteries (10 cm/sec) or capillaries (0.05 cm/sec), the magnetic particles are retained at the target site by the external magnetic field. Once the drug/carrier is concentrated at the targeted location, the drug can be released either via enzymatic activity or changes in physiological conditions such as pH, osmolality, or temperature, and may be internalized by cells of the target tissue or tumor cells. Cytotoxic drugs are concentrated in specific organs and may be combined with cellular and subcellular targeting by tailored surface engineering of the magnetic carriers. This approach, in theory, has major advantages over the normal, non-targeted methods of cytotoxic drug therapy, offering a promising solution to maximize the efficiency of chemotherapy and reduce side-effects. Alexiou *et al.* treated squamous cells carcinoma in rabbits with SPIO loaded with mitoxantrone that was concentrated with an external magnetic field [148]. In the treatment group, the magnetic field was focused on the tumor during SPIO/mitoxantrone infusion for 60 min in total. It was shown that intra-arterial application of SPIO/mitoxantrone with the external magnetic field resulted in a significantly better remission of the squamous cell carcinoma compared with the control group (no treatment) and the intravenous SPIO/mitoxantrone group, with no signs of toxicity [148].

The intravenous injection of magnetic nanocarriers needs to be balanced against a potentially higher RES clearance and requires high energy magnetic fields. The clinical success of magnetic drug targeting depends on strong magnets being able to produce high magnetic field gradients at the target sites. For intravenous administration, magnetic targeting is likely to be most effective in regions of slower blood flow, particularly if the target site is closer to the magnet source. It has been suggested that the use of magnetically targeted drug delivery with an externally applied field is appropriate only for targets close to the surface of the body [149]. Recently, a

novel magnetic drug targeting concept has been proposed. Magnetic nanocarriers encapsulated with a drug are intravenously administered and these magnetic nanocarriers are localized at the target site utilizing an implanted, magnetizable intraluminal stent or seed, such leading to focal high concentration of the drug. Such procedures can be performed on demand acutely or magnetizable seeds are planted chronically [150]. Kubo *et al.* [151] implanted permanent magnets at solid osteosarcoma sites in hamsters and delivered the cytotoxic compounds via magnetic liposomes. This method resulted in a four-fold increase in cytotoxic drug delivery to the osteosarcoma sites when compared with normal intravenous (non-magnetic) delivery. Results also showed a significant increase in anti-tumor activity. The implant-based drug delivery system can also function by the placement of a weakly magnetizable stent (or other implant) at precise locations in the cardiovascular system, followed by the delivery of magnetically susceptible drug carriers. The stents are capable of applying high local magnetic field gradients within the body. The local gradients produced within the blood vessel create the forces needed to attract and hold drug-containing magnetic nanoparticles at the implant site [152]. Theoretical simulations and experimental results support the assumption that using magnetic implants in combination with an externally applied magnetic field will optimize the delivery of a drug to the selected sites [153]. Magnetically controlled drug targeting has been carried out in patients with advanced and unsuccessfully pretreated cancers or sarcomas. Magnetic field strengths of at least 0.5 T and in general 0.8 T can be achieved and confirmed at the patient's bed [154-155].

Successful drug targeting with SPIOs can utilize expensive drugs, and those with a short half-life or a high toxicity. Drugs such as antibiotics, thrombolytic agents, can also be bound reversibly to the SPIOs. Inada *et al.* [156] performed *in-vitro* investigations of localized fibrinolysis by magnetically concentrating urokinase-

magnetite complexes. Thermosensitive magnetoliposomes (TM) have also been prepared and investigated in an *in-vitro* flow system. The TMs with a diameter of about 1 μm could be concentrated in relatively high field strengths. It was possible to release a specific part of the content from the particles (calcein) by increasing the temperature above 40°C [157].

To void the RES clearance, large drug/SPIO composites are delivered intra-arterially [156]. We proposed an SPIO nanoshell based chemoembolization composite for transcatheter anticancer drug delivery, particularly for liver malignancies (Figs. 8, 9). For developing the chemoembolization composite, hollow SPIO nanoshells (150-200nm diameter, the same as in Fig. 7), anticancer drug doxorubicin, and PVA polymers are used. Doxorubicin is encapsulated in the SPIO nanoshells, and the PVA polymers glue SPIO nanoshells together to form embolic particles of 0.5~1mm. The ratio of PVA80 and PVA98 is optimized to control the disintegration rate of PVA polymers in liquid. These SPIO/doxorubicin/PVA composite particles are delivered through a catheter selectively placed in a feeding artery of a tumor [159]. The composite particles are released from the catheter, which then block the feeding artery of the tumor. After a period of time (in days), upon the disintegration of PVA polymers, SPIO nanoshells are released and start moving downstream. Thereafter SPIO nanoshells can be transferred through the leaky tumor vasculature into the tumor tissue, and the anti-tumor drugs are released within the tumor. *In vitro* drug release study showed that doxorubicin loaded in the SPIO nanoshell released gradually from the composite. Due to the magnetic properties of SPIOs, this composite has magnetic drug targeting and MRI contrast potentials.

7. SPIO NANOPARTICLE MEDIATED HYPERTHERMIA THERAPY

The rationale for using hyperthermia in cancer therapy is that sustained temperatures increase above 43°C causes necrosis of cancer cells, which are more heat sensitive than normal tissues. The conditions for hyperthermia thermal ablation therapy are dependent

on the operating temperature and time. Four to six minutes are sufficient at 50-52 °C to induce irreversible cellular damage [160-161]. Being a physical treatment, hyperthermia may result in fewer side effects than chemo- or radiotherapy. SPIO-mediated hyperthermia is based on the unique property of superparamagnetic crystals of iron oxides to absorb the energy of an oscillating magnetic field (100 - 400 kHz) and to convert this energy into heat [17]. Magnetic-nanoparticle-mediated hyperthermia involves targeting SPIO to tumor tissue and then applying an external alternating magnetic field to generate heat. Magnetite (Fe_3O_4) and maghemite ($\gamma\text{-Fe}_2\text{O}_3$) particles are the two types of SPIO used for hyperthermia. Maghemite is produced by the oxidation of magnetite above 300°C and the steps required to produce magnetite are simpler than those required to produce maghemite. Therefore, most studies of sub-micron magnetic particles for issue hyperthermia have focused on magnetite.

Experimentally, many researchers reported encouraging results using hyperthermia with magnetic nanoparticles, such as magnetite-core dextran nanoparticles and aminosilane-coated magnetite. In these therapeutic experiments, magnetites were injected into solid tumors and the animals were irradiated with an alternating magnetic field. After irradiation with the alternating magnetic field, the tumor volume decreased markedly and complete tumor regression was observed in some of the animals. Magnetic materials suitable for hyperthermia are discussed by Atsumi *et al.* in terms of their magnetic properties, practical limitations in treatment conditions, and the instruments used to activate the magnetic particles [162]. Considering the magnetic properties and biocompatibility of the particles, superparamagnetic magnetite with a diameter of 11–13 nm is considered suitable. In the case of magnetite cationic liposomes (MCLs), an accumulation of magnetite nanoparticles inside the tumor cells can be enhanced by conferring a positive surface charge to the liposomal surface (a tenfold higher affinity for glioma cells than neutrally charged magnetoliposomes) [163].

To enhance specific accumulation of SPIOs at the tumor site, antibody-conjugated liposomes containing magnetite nanoparticles

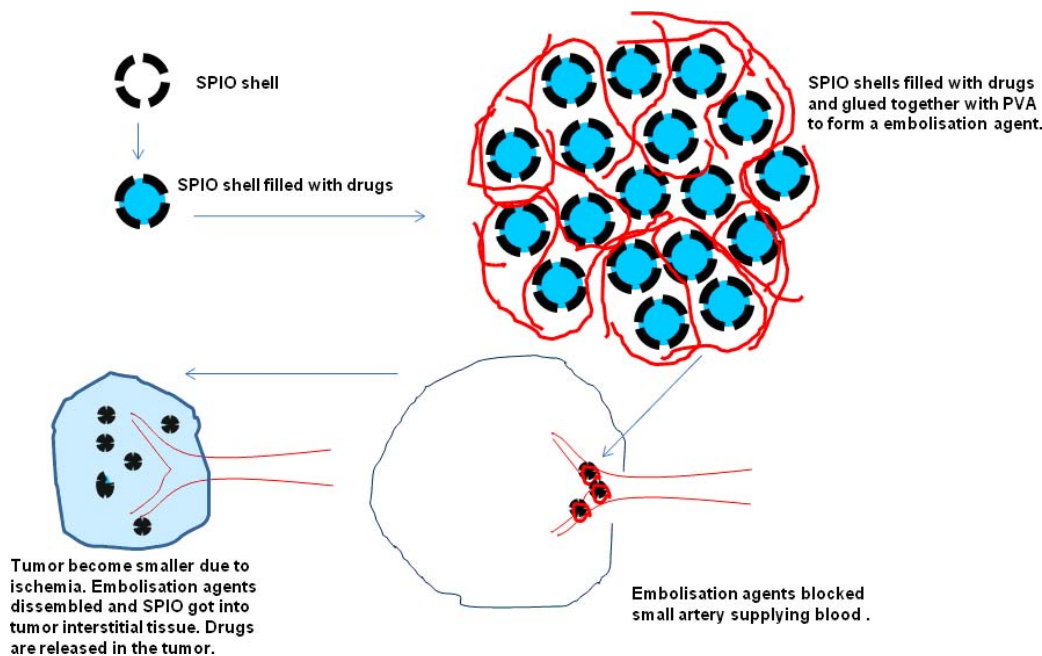


Fig. (8). Schematic diagram of hollow SPIO nanoshell based chemoembolization composites for transcatheter anticancer drug delivery. Step 1: synthesis of hollow SPIO nanoshells; Step 2: encapsulation of anti-cancer drug into the SPIO nanoshells; Step 3: formation of anti-cancer drug filled SPIO nanoshells with PVA to become 0.5~1mm chemoembolization composites; Step 4: chemoembolization composites delivered through a catheter to embolize the arteries supplying blood to the tumor; Step 5: After a period of time, chemoembolization composite dissembled and SPIO nanoshell passed through the leaky tumor vasculature into the tumor tissue, and the anti-tumor drugs were released within the tumor (reproduced with permission from reference 159).

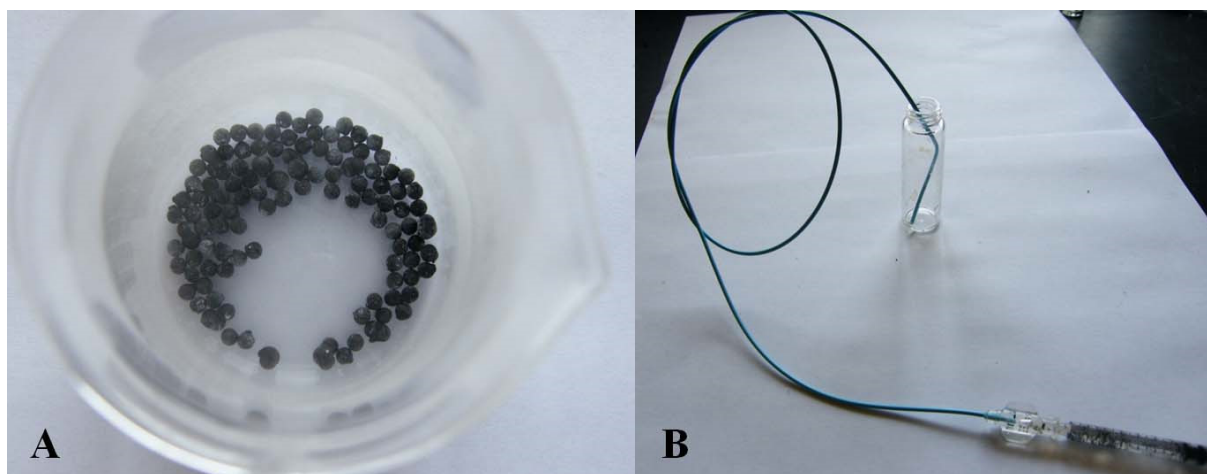


Fig. (9). A: SPIO embolization particles containing nanoshell/doxorubicin/PVA composites B: Composite embolization particles being passed through a catheter for selective hepatic artery drug delivery.

(antibody-conjugated magnetoliposomes, AMLs; core diameter, 10 nm) have been developed. AMLs were constructed by using mouse G22 monoclonal antibodies (mAb) against human glioma cells [164], mouse G250 mAb against human renal cell carcinomas [165], humanized mAb against human epidermal growth factor receptor-2 (HER2; Herceptin) [166], and mAb against human high-molecular-weight melanoma-associated antigen (HMW-MAA). The tumor-specific targeting ability of these AMLs has been demonstrated [8,165]. However, intravenous application of antibody-conjugated magnetoliposomes still does not lead to enough concentration of SPIOs to be applicable for local hyperthermia [167].

In addition to the expected tumor cell death, hyperthermia treatment can also induce unexpected biological responses, such as tumor-specific immune responses as a result of heat-shock protein expression. Hyperthermia has the ability to kill not only local tumors exposed to heat treatment, but also tumors at distant sites, such as metastatic cancer cells. Yanase *et al.* reported anti-tumor immunity resulting from hyperthermia in an experimental T-9 rat glioma model in which T-9 cells were transplanted into the femur of rats used in the experiments [168]. Although only one tumor was subjected to hyperthermia, the other tumor also disappeared completely. An immunohistochemical assay revealed that natural killer (NK) cells and CD8⁺ and CD4⁺ T cells migrated not only into the heated tumor but also into the unheated counterpart.

So-called “smart” systems consisting of a magnetic core for heat production and a multi-stimuli sensitive shell, such as pH- and thermo-sensitive polymers (e.g., block copolymers and copolymer hydrogels) have been proposed. The localized and triggered treatments can enhance the hyperthermia treatment potential by delivering the drugs to the targeted sites. The drug is loaded in the stimulus sensitive shell. Upon reaching the targeted site, the temperature of magnetic core is increased, leading to the structural/conformational changes (e.g., breaking of covalent or non-covalent chemical bonds) in the thermo-sensitive polymeric shell. Consequently, the drug is released locally in the targeted site [169]. These drug delivery systems are promising for future multifunctional chemotherapeutic applications that combine drug release and magnetic hyperthermia therapy.

In 2005, Johannsen *et al.* [170] described the first clinical application of magnetite-nanoparticle-mediated hyperthermia in locally recurrent prostate cancer. In this study, the feasibility of hyperthermia was evaluated by using aminosilane coated magnetite nanoparticles. The nanoparticles were injected transperitoneally into the prostate of a 67-year-old patient under transrectal ultrasound and fluoroscopy guidance. Treatments were performed using an alter-

nating magnetic field of 100 kHz. In this patient, the maximum and minimum intraprostatic temperatures were found to be 48.5 and 40.0°C during the first treatment and 42.5 and 39.4°C during the sixth treatment. Further clinical trials on magnetic-nanoparticle-mediated hyperthermia are on-going [8].

Hepatocellular carcinoma can be a potential target for thermoembolization technique based on targeted deposition of magnetic nanoparticles suspended in Lipiodol into the tumor, followed by application of an alternating current magnetic field inducing focused heating. Selective embolization of VX2 tumor implanted in the liver of rabbits showed initial promising results [171]. However, further investigations from the same team evidenced the presence of ischaemic necrosis in healthy liver parenchyma associated with extensive phagocytosis of nanoparticles [172]. There was no hepatic clearance of the suspension 28 days after injection. Microvascular occlusion was also observed [173]. Despite these data, thermoembolization or thermochemoembolization where a cytotoxic drug is associated remains an active field of research.

8. OTHER APPLICATIONS OF SPIO NANOPARTICLES

8.1. Magnetofection and Gene Delivery

Gene therapy is a promising medical treatment for many diseases including genetic disorders and degenerative diseases. The mechanism of gene therapy is to correct the genetic disorder or produce exogenous proteins/peptides by insertion of exogenous DNA. Gene therapy requires efficient gene delivery vectors, while currently the transfection/transduction efficiency of both viral and non-viral vectors is limited. Magnetic micro- and nanoparticle-based techniques show potential for high-efficiency transfection both *in-vitro* and *in-vivo* [174]. This technique, in which DNA, or viral vectors containing DNA, is attached to a magnetic micro- or nanoparticle carrier, was first developed by Mah *et al.* [175]. It has since been further developed, primarily for *in-vitro*, non-viral applications [176]. In one example, the gene vector was attached to poly(ethylene imine) (PEI) coated SPIOs. The PEI-coated SPIO/vector complexes were tested *in-vitro*, in which a strong permanent magnet was positioned beneath the cell monolayer. Peak transfection levels were achieved with 10-min incubation of cells, compared with 2 to 4 hrs required for other non-viral agents, such as cationic lipids [177].

The feasibility of combining small interfering RNA (siRNA) therapy and *in vivo* monitoring of transplanted islets in mice has been reported, and a protective effect of SPIO-small interfering (si) Caspase-3 in treated islets both *in vitro* and *in vivo* was observed [178]. In addition, a dual-purpose therapy/imaging siRNA SPIO

probe that targets β (2) microglobulin (B2M), a key component of the major histocompatibility class I complex has been proposed. Besides serving as a siRNA carrier, this SPIO-siB2M probe also enables monitoring of graft persistence noninvasively using MRI. Human islets labeled with these SPIOs before transplantation into B2M (null) NOD/scid mice showed significantly improved preservation of graft volume starting at 2 weeks, as determined by longitudinal MRI in an adoptive transfer model. Furthermore, animals transplanted with SPIO-siB2M-labeled islets demonstrated a significant delay of up to 23.8 ± 4.8 days in diabetes onset after the adoptive transfer of T cells relative to 6.5 ± 4.5 days in controls. Therefore these approaches could protect pancreatic islet grafts from immune rejection and could potentially be applied to allotransplantation and prevention of the autoimmune recurrence of type 1 diabetes mellitus in islet transplantation or endogenous islets [179].

8.2. Targeted Delivery and Retention of Magnetizable Stem Cells

When cells, such as stem cells, are labeled by SPIOs, these cells become magnetizable. These magnetizable stem cells labeled with SPIOs can be delivered in a targeted way or can be retained in a desired location. In a pilot study, we validated magnetic targeted transcatheter SPIO labeled stem cell delivery in a rat intracerebral haemorrhage (ICH) model. MSCs were labeled with small polyhedral SPIOs (~10 nm) coated with a thin layer of silica and with surface modification by amines [86]. Rat ICH was induced by stereotactic injection of collagenase into the right side striatum. MSCs delivery was carried out 3 days after ICH induction via a cannula placed in the right internal carotid artery. For five rats, a permanent magnet was placed over the right head of the rats during the MSCs delivery and for additional 20 min post delivery. For another five rats, no external magnet was applied. The preliminary results suggested that magnetic targeting increased MSCs local homing and seeding in the lesion site of the rat ICH model [180].

The success of cardiac stem cell therapies is limited by low cell retention, due in part to the washout via coronary veins. Cheng *et al.* [181] sought to counter the efflux of transplanted cells by rendering them magnetically responsive and imposing an external magnetic field on the heart during and immediately after injection.

In their study, cardiosphere-derived cells (CDCs) were labeled with SPIOs. SPIOs labeled CDCs were injected intramyocardially, with and without a superimposed magnet. With magnetic targeting, cells were visibly attracted toward the magnet and accumulated around the ischemic zone. In contrast, the majority of nontargeted cells washed out immediately after injection. They concluded that magnetic targeting enhances cell retention, engraftment and offers functional benefit [181].

8.3. Carbon Coated Superparamagnetic Iron Oxide Nanoparticles for Sentinel Lymph Nodes Mapping

Intra-operative lymphatic mapping and sentinel lymphadenectomy (LM/SL) map the lymphatic path from the primary tumor to the regional nodes and permit selective excision of the first sentinel lymph nodes. It is a well established technique to detect occult regional node metastases for melanoma patients and breast cancer patients. In continuing attempts to improve accuracy, most surgeons now combine a dye (such as carbon particles) and radiopharmaceuticals when performing LM/SL. We developed a prototype of carbon coated superparamagnetic iron oxide nanoparticles (SPIO@C) for sentinel lymph nodes mapping (Fig. 10) [182]. Compared with combining carbon particles and radiopharmaceuticals for performing LM/SL, there are a number of advantages with our approach: 1) SPIO is an MRI contrast agent, thus pre-operative MRI may be used for LM/SL instead of gamma camera. There is no radiation associated with MRI, and MRI offers good tissue contrast and detailed cross-sectional images. 2) There will be needed only one injection of SPIO@C nanoparticles, instead of administering two successive injections of radiopharmaceuticals and carbon particles. 3) During the operation, an intraoperative MRI scanner can be used, or more conveniently, SPIO detection can be performed with a simple magnetometer.

8.4. Magnetic Nanoparticle Applications in Tissue Engineering

Combining magnetic fields and nanoparticles for tissue engineering applications includes control of cell behavior through magnetic force targeting and cell orientation and mobilization strategies for *in-vitro* generation of tissues [183-185]. Specific mechano-responsive receptors can be tagged on cells, and then magnetic fields can be applied to generate a localized force onto the receptor which results in activation and downstream changes in cell signal-

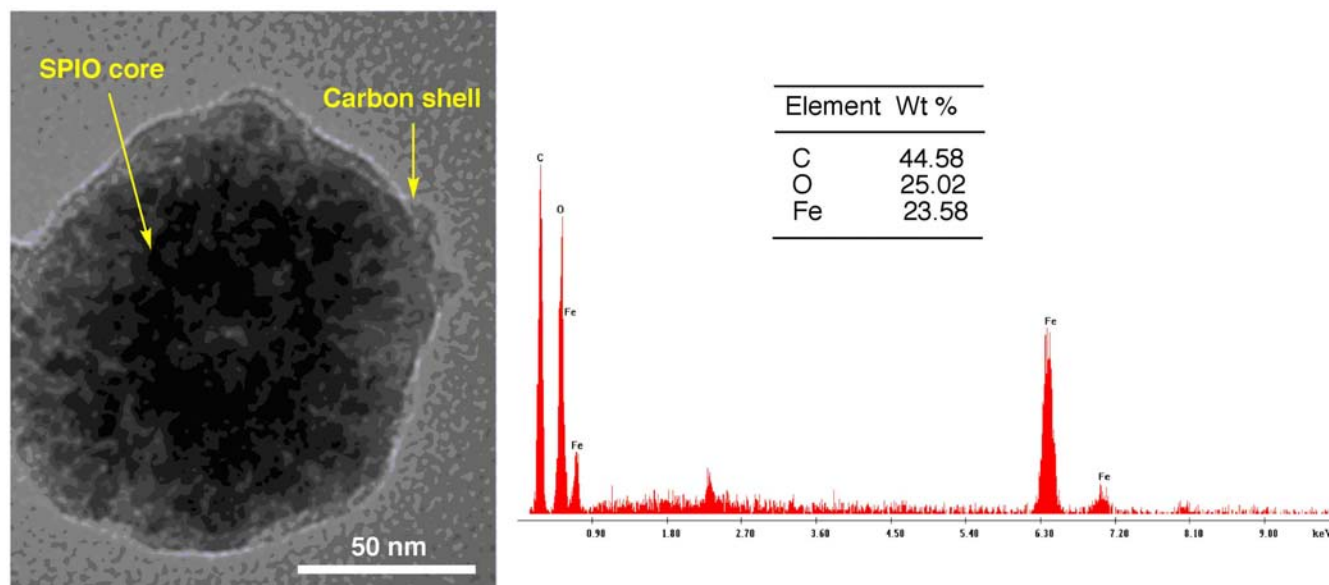


Fig. (10). TEM image (Left) and Energy-dispersive X-ray spectroscopy spectrum (Right) of the SPIO@C nanoparticle (reproduced with permission from reference 182).

ing and ultimately phenotype. This technique is being explored both *in-vivo* and *in-vitro* for stem cell conditioning and new methods for applying mechanical strain to 2-D and 3-D cultures *in-vitro* using a magnetic force bioreactor. Using nanoparticle-labeled cells in scaffolds, magnetic fields can be used to draw the cells through 3-D systems and to form orientated layers [186]. This technique has been considered for endothelial, bone and other tissue applications [187-188].

9. CONCLUSION AND FUTURE PERSPECTIVE

With respect to their potential for drug delivery, SPIOs are typical tools for theranostics which allow the combined diagnosis, treatment and follow up of a disease [189]. SPIO labeled macrophage infiltration can also serve as a surrogate marker for stem cell viability [190, 191]. Theranostics has emerged as a very fast-evolving research area, especially in the field of oncology. This innovative approach allows the characterization of the disease lesion which may lead to select another drug if the target of interest is not expressed, monitoring the local delivery kinetics and following up the efficacy of the treatment on a rational basis. The minimum dosage required for Gd-based targeted contrast agent can be much higher than the appropriate therapeutic dose [189]. Such discrepancy is less preoccupying for iron oxide nanoparticles. Furthermore, local hyperthermia-based therapies allow to take advantage of the specific behavior of SPIO crystals in the presence of an external alternating magnetic field. An important issue needs to be considered when selecting SPIOs for drug delivery is their fate after the drug delivery, i.e. elimination route or retention time in the body system if they are biodegradable and their putative relevant side effects. For example, coated SPIOs could be biocompatible; however, if the iron oxide core is exposed, it may cause an oxidative stress which depends on the coating and the size of SPIOs as well as the type of cells [192].

The business model of SPIOs designed for both follow-up imaging and drug delivery remains to be defined. It is worth noticing that the development process for contrast agents follows the same regulatory rules as therapeutic pharmaceuticals, in term of registration, i.e. the need of pharmaceutical, preclinical and clinical studies is basically similar, with a time to market *also* being roughly similar. This implies long time-to-market and high development budgets. The question remains how to share the value generated between companies involved in medical imaging which generally market "single-use contrast agents" and therapeutic drug companies who focus on a long term access to the market for a high cost treatment. The associated risks for diagnostic companies, which have a much lower return on investment for their products than therapeutic drug companies, should be underlined. A key challenge is the current lack of regulatory guidance for co-development of therapeutic drugs and diagnostic agents. One central issue is whether it is possible to obtain regulatory approval of a diagnostic contrast agent by providing the authorities with similar data as those stemmed from clinical trials performed to support a therapeutic drug approval [193]. An integrated translational approach involving clinicians at an early stage of the projects is the most appropriate way to assess suitability of such projects for a personalized healthcare approach. Like therapeutic drugs, the development of cellular or molecular imaging contrast agents obviously depends on the clinical validation of the biological target. SPIOs could be used as a) prognostic biomarkers if imaging is performed before therapy, for example to investigate the inflammatory involvement; or b) to measure pharmacodynamics response of a treatment. Inhibition of a molecular target such as VEGFR or HER2/*neu* and molecular imaging of the drug interaction at the level of its molecular target represent examples of this second approach. SPIO based imaging can also be used as surrogate endpoint biomarkers during clinical trials or in clinical practice [194, 195]. It is admitted that the traditional criteria (World Health Organization tumor response criteria or the Response Evaluation Criteria for Solid Tumor [RECIST]), based on anatomi-

cal measurements, may miss important consequences of tumor response to new drugs [196]. However, as requested by health authorities, biomarker candidates need to be qualified and validated [194-196]. This obvious obligation led companies involved in discovery and development of therapeutic molecules and those developing contrast agents to collaborate on research projects. Interestingly, the SPIO ferumoxytol is marketed in the US (tradename Feraheme[®]) and has been approved in Europe (Rienso[®]) for the treatment of iron deficiency in adult chronic kidney disease patients. However, this compound is not approved for imaging purposes.

CONFLICT OF INTEREST

Dr Marc Port and Dr Jean-Marc Idee are employees of Guerbet group which develops SPIO agents for clinical application.

ACKNOWLEDGEMENTS

The work is supported partially by a grant from the Research Grants Council of the Hong Kong SAR (Project No.SEG_CUHK02). The authors thank Dr Xiao-Ming Zhu for some of the work described in this paper.

ABBREVIATIONS

SPIO	=	Superparamagnetic iron oxide
MRI	=	Magnetic resonance imaging
PEG	=	Polyethylene glycol
PAA	=	Polyacrylic acid
PVA	=	poly(vinyl alcohol)
PEI	=	Polyethyleneimine
Ms	=	Magnetic saturation value
PVP	=	Polyvinylpyrrolidone
PAA	=	Polyacrylic acid
TEM	=	Transmission electron microscopy
DEG	=	Diethylene glycol
LIPUS	=	Low-intensity pulsed ultrasound
MPIO	=	Micrometer-sized iron oxide particles
RES	=	Reticuloendothelial system
FDG	=	Fluorodeoxyglucose
PET	=	Positron emission tomography
EGFR	=	Epidermal growth factor receptor
VCAM-1	=	Vascular cell adhesion molecule 1
CBV _{ss}	=	Steady-state cerebral blood volume
MIONs	=	Monocrystalline iron oxide nanoparticles
EPR	=	Enhanced permeability and retention
PEGF	=	poly(ethylene glycol)-co-fumarate
TM	=	Thermosensitive magnetoliposomes
MCLs	=	Magnetite cationic liposomes
AMLs	=	Antibody-conjugated magnetoliposomes
mAb	=	Monoclonal antibodies
HMW-MAA	=	High-molecular-weight melanoma-associated antigen
PEI	=	polyethyleneimine
siRNA	=	small interfering RNA
B2M	=	β(2) microglobulin
ICH	=	Intracerebral haemorrhage
CDCs	=	Cardiosphere-derived cells
LM/SL	=	Lymphatic mapping and sentinel lymphadenectomy

HER2	=	Human epidermal growth factor receptor 2
VEGF	=	Vascular endothelial growth factor receptors
RECIST	=	Response evaluation criteria for solid tumor

REFERENCES

- Gupta AK, Gupta M. Synthesis and surface engineering of iron oxide nanoparticles for biomedical applications. *Biomaterials* 2005; 26: 3995–4021.
- Wang YX, Hussain SM, Krestin GP. Superparamagnetic iron oxide contrast agents: physicochemical characteristics and applications in MR imaging. *Eur Radiol* 2001; 11: 2319-31.
- Corot C, Robert P, Idee JM, Port M. Recent advances in iron oxide nanocrystal technology for medical imaging. *Adv Drug Deliv Rev* 2006; 58: 1471-1504.
- Wang YX. Superparamagnetic iron oxide based MRI contrast agents: current status of clinical application. *Quant Imaging Med Surg* 2011; 1: 35-40.
- Bulte JW, Kraitchman DL. Monitoring cell therapy using iron oxide MR contrast agents. *Curr Pharm Biotechnol* 2004; 5: 567-84.
- Daldrup-Link HE, Rudelius M, Piontek G, *et al.* Migration of iron oxide-labeled human hematopoietic progenitor cells in a mouse model: *in vivo* monitoring with 1.5-T MR imaging equipment. *Radiology* 2005; 234: 197-205.
- Xu H, Aguilar ZP, Yang L, Kuang M, Duan H, Xiong Y, Wei H, Wang A. Antibody conjugated magnetic iron oxide nanoparticles for cancer cell separation in fresh whole blood. *Biomaterials* 2011; 32: 9758-65.
- Kobayashi T. Cancer hyperthermia using magnetic nanoparticles. *Biotechnol. J* 2011; 6: 1342-7.
- Mahmoudi M, Sant S, Wang B, Laurent S, Sen T. Superparamagnetic iron oxide nanoparticles (SPIONs): development, surface modification and applications in chemotherapy. *Adv Drug Deliv Rev* 2011; 63: 24-46.
- McBain SC, Yiu HH, Dobson J. Magnetic nanoparticles for gene and drug delivery. *Int J Nanomedicine* 2008; 3: 169-80.
- Jain TK, Morales MA, Sahoo SK, Leslie-Pelecky DL, Labhasetwar V. Iron oxide nanoparticles for sustained delivery of anticancer agents. *Mol Pharm* 2005; 2: 194-205.
- Thorek DL, Chen AK, Czupryna J, Tsourkas A. Superparamagnetic iron oxide nanoparticle probes for molecular imaging. *Ann Biomed Eng* 2006; 34: 23-38
- Lu AH, Salabas EL, Schuth F. Magnetic nanoparticles: synthesis, protection, functionalization, and application. *Angew. Chem. Int. Ed* 2007; 46: 1222–4.
- Welo LA, Baudisch B. The two-stage transformation of magnetic into hematite. *Philos. Mag* 1925; 50: 399-408.
- Qiao R, Yang C, Gao M. Superparamagnetic iron oxide nanoparticles: from preparations to *in vivo* MRI applications. *J. Mater. Chem* 2009; 19: 6274-93.
- Wang Z, Guo H, Yu Y, He N. Carbon-coated iron oxide nanoparticles as contrast agents in magnetic resonance imaging. *Magn. Mater* 2006; 302: 397-404.
- Laurent S, Forge D, Port M, *et al.* Magnetic iron oxide nanoparticles: synthesis, stabilization, vectorization, physicochemical characterizations, and biological applications. *Chem Rev* 2008; 108: 2064-110.
- Wang J, Sun J, Sun Q, Chen Q. One-step hydrothermal process to prepare highly crystalline Fe₃O₄ nanoparticles with improved magnetic properties. *Mater. Res. Bul* 2003; 38: 1113-8.
- Xuan S, Hao L, Jiang W, Gong X, Hu Y, Chen Z. Preparation of water-soluble magnetic nanocrystals through hydrothermal approach. *J. Magn. Mater* 2007; 308: 210-3.
- Si S, Li C, Wang X, *et al.* Magnetic monodisperse Fe₃O₄ nanoparticles. *Crystal Growth Design* 2005; 5: 391-3.
- Zhang L, Qiao S, Jin Y, *et al.* Fabrication and size-selective bioseparation of magnetic silica nanospheres with highly ordered periodic mesostructure. *Adv. Funct. Mater* 2008; 18: 3203-12.
- Peng X, Wickham J, Alivisatos A.P. Kinetics of II-VI and III-V colloidal semiconductor nanocrystal growth: “focusing” of size distributions. *J. Am. Chem. Soc* 1998; 120: 5343-4.
- O'Brien S, Brus L, Murray CB. Synthesis of monodisperse nanoparticles of barium titanate: toward a generalized strategy of oxide nanoparticle synthesis. *J. Am. Chem. Soc* 2001; 123: 12085-6.
- Sun S, Zeng H. Size-Controlled Synthesis of Magnetite Nanoparticles. *J. Am. Chem. Soc* 2002; 124: 8204-5.
- Park J, An K, Hwang Y, *et al.* Ultra-large-scale syntheses of monodisperse nanocrystals. *Nat. Mater* 2004; 3: 891-5.
- Park J, Lee E, Hwang NM, *et al.* One-nanometer-scale size-controlled synthesis of monodisperse magnetic iron oxide nanoparticles. *Angew. Chem. Int. Ed* 2005; 44: 2872–7.
- Li Z, Chen H, Bao H, Gao M. One-Pot Reaction to Synthesize Water-Soluble Magnetite Nanocrystals. *Chem. Mater* 2004; 16: 1391-3.
- Li Z, Sun Q, Gao M. Preparation of Water-Soluble Magnetite Nanocrystals from Hydrated Ferric Salts in 2-Pyrrolidone: Mechanism Leading to Fe₃O₄. *Angew. Chem. Int. Ed.*, 2005; 44: 123-6
- Jana NR, Chen Y, Peng X. Size- and shape-controlled magnetic (Cr, Mn, Fe, Co, Ni) oxide nanocrystals via a simple and general approach. *Chem. Mater* 2004; 16: 3931-5.
- Ge JP, Hu Y, Biasini M, Beyermann WP, Yin Y. Superparamagnetic magnetite colloidal nanocrystal clusters. *Angew. Chem. Int. Ed* 2007; 46: 4342-5.
- Deng H, Li X, Peng Q, Wang X, Chen J, Li Y. Monodisperse magnetic single-crystal ferrite microspheres. *Angew. Chem. Int. Ed* 2005; 44: 2782-5.
- Liu J, Sun Z, Deng Y, *et al.* Colloids highly water-dispersible biocompatible magnetite particles with low cytotoxicity stabilized by citrate groups. *Angew. Chem. Int. Ed* 2009; 48: 5875–9.
- Xuan S, Wang F, Wang YX, Yu JC, Leung KC. Facile synthesis of size-controllable monodispersed ferrite nanospheres. *J. Mater. Chem* 2010; 20: 5086-94.
- Liu C, Zou B, Rondinone AJ, Zhang ZJ. Reverse Micelle Synthesis and Characterization of Superparamagnetic MnFe₂O₄ Spinel Ferrite Nanocrystallites. *J. Phys. Chem* 2000; 104: 1141-5.
- Jia J, Yu JC, Wang YX, Chan KM. Magnetic Nanochains of FeNi(3) Prepared by a Template-Free Microwave-Hydrothermal Method. *ACS Appl. Mater. & Inter* 2010; 2: 2579-84.
- Piao Y, Kim J, Bin Na H, *et al.* Wrap-bake-peel process for nanostructural transformation from b-FeOOH nanorods to biocompatible iron oxide nanocapsules. *Nat Mater* 2008; 7: 242-7
- Zhang WM, Wu XL, Hu JS, Guo YS, Wan LJ. Carbon Coated Fe₃O₄ Nanospindles as a Superior Anode Material for Lithium-Ion Batteries. *Adv. Funct. Mater* 2008; 18: 3941-6.
- Cheng W, Tang K, Qi Y, Sheng J, Liu Z. One-step synthesis of superparamagnetic monodisperse porous Fe₃O₄ hollow and core-shell spheres. *J. Mater. Chem* 2010; 20: 1799-1805.
- Xuan S, Wang F, Lai JM, *et al.* Synthesis of biocompatible, mesoporous Fe(3)O(4) nano/microspheres with large surface area for magnetic resonance imaging and therapeutic applications. *ACS Appl. Mater. & Inter* 2011; 3: 237-44.
- Leung KC, Wang YX, Wang HH, Chak CP, Cheng CH. Biological and magnetic contrast evaluation of shape-selective Mn–Fe nanowires. *IEEE Transactions on Nanobioscience* 2009; 8: 192-8.
- Jia J, Yu JC, Zhu XM, Chan KM, Wang YX. An ultra-fast method to synthesize mesoporous magnetite nanoclusters as highly sensitive magnetic resonance probe. *J Colloid Interface Sci* 2012; 379: 1-7.
- Mohapatra S, Pramanik N, Ghosh SK, Pramanik P. Synthesis and characterization of ultrafine poly(vinylalcohol phosphate) coated magnetite nanoparticles. *J. Nanosci. Nanotechnol* 2006; 6: 823-9.
- Lu X, Niu M, Qiao R, Gao M. Superdispersible PVP-coated Fe₃O₄ nanocrystals prepared by a "one-pot" reaction. *J. Phys. Chem. B* 2008; 112: 14390-4.
- Moghimi SM, Hunter AC. Recognition by macrophages and liver cells of opsonized phospholipid vesicles and phospholipid head-groups. *Pharm. Res* 2001; 18: 1-8.
- Di Marco M, Port M, Couvreur P, Dubernet C, Ballirano P, Sadun C. Structural characterization of ultrasmall superparamagnetic iron oxide (USPIO) particles in aqueous suspension by energy dispersive X-ray diffraction (EDXD). *J Am Chem Soc* 2006; 128: 10054-9.
- Pellegrino T, Manna L, Kudara S, *et al.* Hydrophobic nanocrystals coated with an amphiphilic polymer shell: A general route to water soluble nanocrystals. *Nano Lett* 2004; 4: 703-7.
- Zhang T, Ge J, Hu Y, Yin Y. A general approach for transferring hydrophobic nanocrystals into water. *Nano Lett* 2007; 7: 3203-7.
- Bai F, Wang D, Huo Z, *et al.* A versatile bottom-up assembly approach to colloidal spheres from nanocrystals. *Angew. Chem. Int. Ed* 2007; 46: 6650-3.

- [50] Zhuang J, Wu H, Yang Y, Cao Y. Controlling colloidal superparticle growth through solvophobic interactions. *Angew. Chem. Int. Ed* 2008; 47: 2208-12.
- [51] Im SH, Herricks T, Lee YT, Xia YN. Synthesis and characterization of monodisperse silica colloids loaded with superparamagnetic iron oxide nanoparticles. *Chem. Phys. Lett* 2005; 401: 19-23.
- [52] Ge J, He L, Goebel J, Yin Y. Assembly of Magnetically Tunable Photonic Crystals in Nonpolar Solvents. *J. Am. Chem. Soc* 2009; 131: 3484-6.
- [53] Ge J, Hu Y, Zhang T, Yin, Y. Superparamagnetic Composite colloids with anisotropic structures. *J. Am. Chem. Soc* 2007; 129: 8974-5.
- [54] Xu Z, Hou Y, Sun S. Magnetic core/Shell Fe₃O₄/Au and Fe₃O₄/Au/Ag nanoparticles with tunable plasmonic properties. *J. Am. Chem. Soc* 2007; 129: 8698-9.
- [55] Xuan S, Wang YX, Leung KCF, Shu K. Synthesis of Fe₃O₄@polyaniline core/shell microspheres with well-defined blackberry-like morphology. *J. Phys. Chem. C* 2008; 112: 18804-9.
- [56] Xuan S, Wang YX, Yu JC, Leung KC. Preparation, characterization and catalytic activity of core/shell Fe₃O₄@polyaniline@Au nanocomposites. *Langmuir* 2009; 25: 11835-43.
- [57] Vestal CR, Zhang ZJ. Atom transfer radical polymerization synthesis and magnetic characterization of MnFe₂O₄/Polystyrene core/shell nanoparticles. *J. Am. Chem. Soc* 2002; 124: 14312-3.
- [58] Lan F, Liu KX, Jiang W, Zeng XB, Wu Y, Gu ZW. Facile synthesis of monodisperse superparamagnetic Fe₃O₄/PMMA composite nanospheres with high magnetization. *Nanotechnology* 2011; 22: 225604.
- [59] Zhang H, Zhong X, Xu JJ, Chen HY. Fe₃O₄/Polypyrrole/Au nanocomposites with core/shell structure: synthesis, characterization, and their electrochemical properties. *Langmuir* 2008; 24: 13748-52.
- [60] You LJ, Xu S, Ma WF, *et al.* Ultrafast hydrothermal synthesis of high quality magnetic core phenol-formaldehyde shell composite microspheres using the microwave method. *Langmuir* 2012; 28: 10565-72.
- [61] Sun X, Li Y. Colloidal carbon spheres and their core/shell structures with Noble-metal nanoparticles. *Angew. Chem. Int. Ed* 2004; 43: 597-601.
- [62] Xuan S, Hao L, Jiang W, Gong X, Hu Y, Chen Z. A facile method to fabricate carbon-encapsulated Fe₃O₄ core/shell composites. *Nanotechnology* 2007; 18: 035602.
- [63] Wang H, Sun YB, Chen QW, Yu YF, Cheng K. Synthesis of carbon-encapsulated superparamagnetic colloidal nanoparticles with magnetic-responsive photonic crystal property. *Dalton Trans* 2010; 39: 9565-9.
- [64] Xie J, Xu C, Kohler N, Hou Y, Sun S. Controlled PEGylation of monodisperse Fe₃O₄ nanoparticles for reduced non-specific uptake by macrophage cells. *Adv. Mater* 2007; 19: 3163-66.
- [65] Wang B, Xu C, Xie J, Yang Z, Sun S. pH controlled release of chromone from chromone-Fe₃O₄ nanoparticles. *J. Am. Chem. Soc* 2008; 130: 14436-7.
- [66] Xu C, Xu K, Gu H, *et al.* Nitrotriacetic acid-modified magnetic nanoparticles as a general agent to bind histidine-tagged proteins. *J. Am. Chem. Soc* 2004; 126: 3392-3.
- [67] Wilhelm C, Billotey C, Roger J, Pons JN, Bacri JC, Gazeau F. Intracellular uptake of anionic superparamagnetic nanoparticles as a function of their surface coating. *Biomaterials* 2003; 24: 1001-11.
- [68] Villanueva A, Cañete M, Roca AG, *et al.* The influence of surface functionalization on the enhanced internalization of magnetic nanoparticles in cancer cells. *Nanotechnology* 2009; 20: 115103.
- [69] Osaka T, Nakanishi T, Shanmugam S, Takahama S, Zhang H. Effect of surface charge of magnetite nanoparticles on their internalization into breast cancer and umbilical vein endothelial cells. *Colloids Surf B Biointerfaces*. 2009; 71: 325-30.
- [70] Corot C, Port M, Guilbert I, *et al.* Superparamagnetic contrast agents. In: *Molecular and Cellular MR Imaging*. Modo MMJ and Bulte JWM (eds), CRC Press, Boca Raton, FL, USA, 2007, 59-83.
- [71] Raynal I, Prigent P, Peyramaure S, Najid A, Rebuzzi C, Corot C. Macrophage endocytosis of superparamagnetic iron oxide nanoparticles: mechanisms and comparison of ferumoxides and ferumoxtran-10. *Invest Radiol* 2004; 39(1): 56-63.
- [72] Chao Y, Parmali PP, Simberg D. Role of carbohydrate receptors in the macrophage uptake of dextran-coated iron oxide nanoparticles. In E. Zahavy *et al.* (eds). *Nano-Biotechnology for Biomedical and Medical Research*. Advances in Experimental Medicine and Biology 2012, Springer-Verlag, 115-123.
- [73] Hogemann D, Josephson L, Weissleder R, Basilion JP. Improvement of MRI probes to allow efficient detection of gene expression. *Bioconjug Chem* 2000; 11(6): 941-6.
- [74] Weissleder R, Moore A, Mahmood U, *et al.* *In vivo* magnetic resonance imaging of transgene expression. *Nat Med* 2000; 6: 351-5.
- [75] Bulte JW, Zhang S, van Gelderen P, *et al.* Neurotransplantation of magnetically labeled oligodendrocyte progenitors: magnetic resonance tracking of cell migration and myelination. *Proc Natl Acad Sci USA* 1999; 96: 15256-61.
- [76] Lewin M, Carlesso N, Tung CH, *et al.* Tat peptide-derivatized magnetic nanoparticles allow *in vivo* tracking and recovery of progenitor cells. *Nat Biotechnol* 2000; 18: 410-4.
- [77] Josephson L, Tung CH, Moore A, Weissleder R. High-efficiency intracellular magnetic labeling with novel superparamagnetic-Tat peptide conjugates. *Bioconjug Chem* 1999; 10: 186-91.
- [78] Dodd CH, Hsu HC, Chu WJ, *et al.* Normal T-cell response and *in vivo* magnetic resonance imaging of T cells loaded with HIV transactivator-peptide-derived superparamagnetic nanoparticles. *J. Immunol Methods* 2001; 256: 89-105.
- [79] Rogers WJ, Meyer CH, Kramer CM. Technology insight: *in vivo* cell tracking by use of MRI. *Nat Clin Pract Cardiovasc Med* 2006; 3: 554-62.
- [80] Strand BL, Ryan TL, In't Veld P, *et al.* Poly-L-Lysine induces fibrosis on alginate microcapsules via the induction of cytokines. *Cell Transplant* 2001; 10: 263-75.
- [81] Metz S, Bonaterra G, Rudelius M, *et al.* Capacity of human monocytes to phagocytose approved iron oxide MR contrast agents *in vitro*. *Eur Radiol* 2004; 14: 1851-8.
- [82] Petri-Fink A, Hofmann H. Superparamagnetic iron oxide nanoparticles (SPIONs): From synthesis to *in vivo* studies - A summary of the synthesis, characterization, *in vitro*, and *in vivo* investigations of SPIONs with particular focus on surface and colloidal properties. *IEEE Trans on Nanobioscience* 2007; 6: 289-97.
- [83] Matuszewski L, Persigehl T, Wall A, *et al.* Cell tagging with clinically approved iron oxides: feasibility and effect of lipofection, particle size, and surface coating on labeling efficiency. *Radiology* 2005; 235: 155-61.
- [84] Thorek DL, Tsourkas A. Size, charge and concentration dependent uptake of iron oxide particles by non-phagocytic cells. *Biomaterials* 2008; 29: 3583-90.
- [85] Zhu XM, Wang YX, Leung KC, *et al.* Enhanced cellular uptake of aminosilane coated superparamagnetic iron oxide nanoparticles in mammalian cell lines. *Int J Nanomedicine* 2012; 7: 953-64.
- [86] Wang HH, Wang YX, Leung KC, *et al.* Durable mesenchymal stem cell labelling using polyhedral superparamagnetic iron oxide nanoparticles. *Chem. Eur. J* 2009; 15: 12417-25.
- [87] Wang YX, Quercy-Jouvet T, Wang HH, *et al.* Efficacy and durability in direct labeling of mesenchymal stem cells using ultrasmall superparamagnetic iron oxide nanoparticles with organosilica, dextran, and PEG coatings. *Materials* 2011; 4: 703-15.
- [88] Wang YX, Leung KC, Cheung WH, *et al.* Low-intensity pulsed ultrasound increases cellular uptake of superparamagnetic iron oxide nanomaterial: results from human osteosarcoma cell line U2OS. *J Magn Reson Imaging* 2010; 31: 1508-13.
- [89] Tanaka T, Sakai R, Kobayashi R, Hatakeyama K, Matsunaga T. Contributions of phosphate to DNA adsorption/desorption behaviors on aminosilane-modified magnetic nanoparticles. *Langmuir* 2009; 25: 2956-61.
- [90] Zhang C, Wangler B, Morgenstern B, *et al.* Silica- and alkoxy-silane-coated ultrasmall superparamagnetic iron oxide particles: a promising tool to label cells for magnetic resonance imaging. *Langmuir* 2007; 23: 1427-34.
- [91] Kunzmann A, Andersson B, Vogt C, *et al.* Efficient internalization of silica-coated iron oxide nanoparticles of different sizes by primary human macrophages and dendritic cells. *Toxicol Appl Pharmacol* 2011; 253: 81-93.
- [92] Hwang YH, Lee DY. Magnetic resonance imaging using heparin-coated superparamagnetic iron oxide nanoparticles for cell tracking *in vivo*. *Quant Imaging Med Surg* 2012; 2: 118-23.
- [93] Lee DY. Highly effective T2 MR contrast agent based on heparinized superparamagnetic iron oxide nanoparticles. *Macromolecular Research* 2011; 19: 843-847.

- [94] Lee JH, Jung MJ, Hwang YH, *et al.* Heparin-coated superparamagnetic iron oxide for *in vivo* MR imaging of human MSCs. *Biomaterials* 2012; 33: 4861-4871.
- [95] Arbab AS, Yocum GT, Kalish H, *et al.* Efficient magnetic cell labeling with protamine sulfate complexed to ferumoxides for cellular MRI. *Blood* 2004; 104: 1217-23.
- [96] Jung MJ, Lee SS, Hwang YH, *et al.* MRI of transplanted surface-labeled pancreatic islets with heparinized superparamagnetic iron oxide nanoparticles. *Biomaterials* 2011; 32: 9391-400.
- [97] Moon HJ, Yun YP, Han CW, *et al.* Effect of heparin and alendronate coating on titanium surfaces on inhibition of osteoclast and enhancement of osteoblast function. *Biochem Biophys Res Commun* 2011; 413: 194-200.
- [98] Shen H, Hu X, Yang F, Bei J, Wang S. Cell affinity for bFGF immobilized heparin-containing poly(lactide-co-glycolide) scaffolds. *Biomaterials* 2011; 32: 3404-12.
- [99] Gozal E, Ortiz LA, Zou X, Burow ME, Lasky JA, Friedman M. Silica-induced apoptosis in murine macrophage: involvement of tumor necrosis factor-alpha and nuclear factor-kappaB activation. *Am J Respir Cell Mol Biol* 2002; 27: 91-8.
- [100] Shapiro EM, Medford-Davis LN, Fahmy TM, Dunbar CE, Koretsky AP. Antibody-mediated cell labeling of peripheral T cells with micron-sized iron oxide particles (MPIOs) allows single cell detection by MRI. *Contrast Media Mol Imaging* 2007; 2: 147-53.
- [101] Weissleder R, Stark DD, Engelstad BL, *et al.* Superparamagnetic iron oxide: pharmacokinetics and toxicity. *Am J Roentgenol* 1989; 152: 167-73.
- [102] Lee JM, Kim IH, Kwak HS, Youk JH, Han YM, Kim CS. Detection of small hypervascular hepatocellular carcinomas in cirrhotic patients: comparison of superparamagnetic iron oxide-enhanced MR imaging with dual-phase spiral CT. *Korean J Radiol* 2003; 4: 1-8.
- [103] Ba-Ssalamah A, Uffmann M, Saini S, Bastati N, Herold C, Schima W. Clinical value of MRI liver-specific contrast agents: a tailored examination for a confident non-invasive diagnosis of focal liver lesions. *Eur Radiol* 2009; 19: 342-57.
- [104] Tanaka M, Nakashima O, Wada Y, Kage M, Kojiro M. Pathomorphological study of Kupffer cells in hepatocellular carcinoma and hyperplastic nodular lesions in the liver. *Hepatology* 1996; 24: 807-12.
- [105] Aguirre DA, Behling CA, Alpert E, Hassanein TI, Sirlin CB. Liver fibrosis: noninvasive diagnosis with double contrast material-enhanced MR imaging. *Radiology* 2006; 239: 425-37.
- [106] Wang YX. Comments on Jing *et al.* original article "In vivo MR imaging tracking of magnetic iron oxide nanoparticle labeled, engineered, autologous bone marrow mesenchymal stem cells following intra-articular injection." *Joint Bone Spine* 2009; 76: 118-9.
- [107] Wang YX, Wang HH, Au DWT, Zuo BS, Teng LS. Pitfalls in employing superparamagnetic iron oxide particles for stem cell labeling and *in vivo* MRI tracking. *Br J Radiol* 2008; 81: 987-8.
- [108] Foster-Gareau P, Heyn C, Alejski A, Rutt BK. Imaging single mammalian cells with a 1.5 T clinical MRI scanner. *Magn Reson Med* 2003; 49: 968-71.
- [109] Shapiro EM, Sharer K, Skrtic S, Koretsky AP. *In vivo* detection of single cells by MRI. *Magn Reson Med* 2006; 55: 242-9.
- [110] Schäfer R, Bantleon R, Kehlbach R, *et al.* Functional investigations on human mesenchymal stem cells exposed to magnetic fields and labeled with clinically approved iron nanoparticles. *BMC Cell Biol* 2010; 11: 22.
- [111] Schäfer R, Kehlbach R, Müller M, *et al.* Labeling of human mesenchymal stromal cells with superparamagnetic iron oxide leads to a decrease in migration capacity and colony formation ability. *Cytotherapy* 2009; 11: 68-78.
- [112] Syková E, Jendelová P. Magnetic resonance tracking of implanted adult and embryonic stem cells in injured brain and spinal cord. *Ann N Y Acad Sci* 2005; 1049: 146-60.
- [113] Sigovan M, Kaye E, Lancelot E, *et al.* Anti-Inflammatory Drug Evaluation in ApoE-Mice by Ultrasmall Superparamagnetic Iron Oxide-Enhanced Magnetic Resonance Imaging. *Invest Radiol* 2012; 47: 546-552.
- [114] Wang YX, Lam WW. Characterisation of brain disorders and evaluation of therapy by functional and molecular magnetic resonance techniques. *Hong Kong Med J* 2008; 14: 469-78.
- [115] Saleh A, Schroeter M, Jonkmanns C, Hartung HP, Mödder U, Jander S. *In vivo* MRI of brain inflammation in human ischaemic stroke. *Brain* 2004; 127: 1670-7.
- [116] Dousset V, Brochet B, Deloire MS, *et al.* MR imaging of relapsing multiple sclerosis patients using ultra-small-particle iron oxide and compared with gadolinium. *Am J Neuroradiol* 2006; 27: 1000-5.
- [117] Neuwelt EA, Várallyay P, Bagó AG, Muldoon LL, Nesbit G, Nixon R. Imaging of iron oxide nanoparticles by MR and light microscopy in patients with malignant brain tumours. *Neuropathol Appl Neurobiol* 2004; 30: 456-71.
- [118] Kooi ME, Cappendijk VC, Cleutjens KB, *et al.* Accumulation of ultrasmall superparamagnetic particles of iron oxide in human atherosclerotic plaques can be detected *in vivo* magnetic resonance imaging. *Circulation* 2003; 107: 2453-8.
- [119] Trivedi RA, Mallawarachi C, U-King-Im JM, *et al.* Identifying inflamed carotid plaques using *in vivo* USPIO-enhanced MR imaging to label plaque macrophages. *Arterioscler. Thromb. Vasc. Biol* 2006; 26: 1601-6.
- [120] Tang T, Howarth SP, Miller SR, *et al.* Assessment of inflammatory burden contralateral to the symptomatic carotid stenosis using high-resolution ultrasmall, superparamagnetic iron oxide-enhanced MRI. *Stroke* 2006; 37: 2266-70.
- [121] Trivedi RA, U-King-Im JM, Graves MJ, *et al.* *In vivo* detection of macrophages in human carotid atheroma: temporal dependence of ultrasmall superparamagnetic particles of iron oxide-enhanced MRI. *Stroke* 2004; 35: 1631-5.
- [122] Tang TY, Howarth SP, Miller SR, *et al.* The ATHEROMA (Atorvastatin Therapy: Effects on Reduction of Macrophage Activity) Study. Evaluation using ultrasmall superparamagnetic iron oxide-enhanced magnetic resonance imaging in carotid disease. *J Am Coll Cardiol* 2009; 53: 2039-50.
- [123] Yancy AD, Olzinski AR, Hu TC, *et al.* Differential uptake of ferumoxtran-10 and ferumoxytol ultrasmall superparamagnetic iron oxide contrast agents in rabbits: critical determinants of atherosclerotic plaque labelling. *J Magn. Reson. Imaging* 2005; 21: 432-42.
- [124] Fayad ZA, Razzouk L, Briley-Saebo KC, Mani V. Iron oxide magnetic resonance imaging for atherosclerosis therapeutic evaluation: still "rusty?". *J Am Coll Cardiol* 2009; 53: 2051-2052.
- [125] Patterson AJ, Tang TY, Graves MJ, Müller KH, Gillard JH. *In vivo* carotid plaque MRI using quantitative T2* measurements with ultrasmall superparamagnetic iron oxide particles: a dose-response study to statin therapy. *NMR Biomed* 2011; 24: 89-95.
- [126] Kinner S, Maderwald S, Parohl N, *et al.* Contrast-enhanced magnetic resonance angiography in rabbits: evaluation of the gadolinium-based agent p846 and the iron-based blood pool agent p904 in comparison with gadoterate meglumine. *Invest Radiol* 2011; 46: 524-529.
- [127] Moeller S, Freiwald WA, Tsao DY. Patches with link: a unified system for processing faces in the macaque temporal lobe. *Science* 2008; 320: 1355-1359.
- [128] Smirnakis SM, Schmid MC, Weber B, Tolia AS, Augath M, Logothetis NK. Spatial specificity of BOLD versus cerebral blood volume fMRI for mapping cortical organization. *J Cereb Blood Flow Metab* 2007; 27: 1248-1261.
- [129] Leite FP, Tsao D, Vanduffel W, Fize D, Sasaki Y, Wald LL, Dale AM, Kwong KK, Orban GA, Rosen BR, Tootell RB, Mandeville JB. Repeated fMRI using iron oxide contrast agent in awake, behaving macaques at 3 Tesla. *Neuroimage* 2002; 16: 283-94.
- [130] Borsook D, Becerra L, Hargreaves R. A role for fMRI in optimizing CNS drug development. *Nat Rev Drug Discov* 2006; 5: 411-424.
- [131] Maeda H, Wu J, Sawa T, Matsumura Y, Hori K. Tumor vascular permeability and the EPR effect in macromolecular therapeutics: a review. *J Control Release* 2000; 65: 271-84.
- [132] Cho K, Wang X, Nie S, Chen ZG, Shin DM. Therapeutic nanoparticles for drug delivery in cancer. *Clin Cancer Res* 2008; 14: 1310-6.
- [133] Stinchcombe TE. Nanoparticle albumin-bound paclitaxel: a novel Cremphor-EL-free formulation of paclitaxel. *Nanomedicine (Lond)* 2007; 2: 415-23.
- [134] Mahmoudi M, Simchi A, Imani M, Hafeli UO. Superparamagnetic iron oxide nanoparticles with rigid cross-linked polyethylene glycol fumarate coating for application in imaging and drug delivery. *J Phys Chem C* 2009; 113: 8124-31.
- [135] Guo S, Li D, Zhang L, Li J, Wang E. Monodisperse mesoporous superparamagnetic single-crystal magnetite nanoparticles for drug delivery. *Biomaterials* 2009; 30: 1881-9.
- [136] Kubo T, Sugita T, Shimose S, Nitta Y, Ikuta Y, Murakami T. Targeted delivery of anticancer drugs with intravenously administered

- magnetic liposomes in osteosarcoma-bearing hamsters. *Int J Oncol* 2000; 17: 309-15.
- [137] Gonzales M, Krishnan KM. Synthesis of magnetoliposomes with monodisperse iron oxide nanocrystal cores for hyperthermia. *J Magn Magn Mater* 2005; 293: 265-70.
- [138] Peppas NA, Hilt JZ, Khademhosseini A, Langer R. Hydrogels in biology and medicine: from molecular principles to bionanotechnology. *Adv Mater* 2006; 18: 1345-60.
- [139] Babincová M, Cicmanec P, Altanerová V, Altaner C, Babinec P. Magnetic field controlled drug release from magnetoliposomes: design of a method for site-specific chemotherapy. *Bioelectrochemistry* 2002; 55: 17-9.
- [140] Patel VR, Agrawal YK. Nanosuspension: An approach to enhance solubility of drugs. *J Adv Pharm Technol Res* 2011; 2: 81-7.
- [141] Jain TK, Foy SP, Erokwu B, Dimitrijevic S, Flask CA, Labhasetwar V. Magnetic resonance imaging of multifunctional pluronic stabilized iron-oxide nanoparticles in tumor-bearing mice. *Biomaterials* 2009; 30: 6748-56.
- [142] Chen Y, Chen H, Zeng D, *et al.* Core/shell structured hollow mesoporous nanocapsules: a potential platform for simultaneous cell imaging and anticancer drug delivery. *ACS Nano* 2010; 4: 6001-13.
- [143] Cheng W, Tang K, Qi Y, Sheng J, Liu Z. One-step synthesis of superparamagnetic monodisperse porous Fe₃O₄ hollow and core-shell spheres. *J. Mater. Chem* 2010; 20: 1799-1805.
- [144] Iram M, Guo C, Guan Y, Ishfaq A, Liu H. Adsorption and magnetic removal of neutral red dye from aqueous solution using Fe₃O₄ hollow nanospheres. *J. Hazard. Mater* 2010; 181: 1039-50.
- [145] Zhu XM, Yuan J, Leung KC, *et al.* Hollow superparamagnetic iron oxide nanoshells as a hydrophobic anticancer drug carrier: intracellular pH-dependent drug release and enhanced cytotoxicity. *Nanoscale* 2012; 4: 5744-54.
- [146] Wilson MW, Kerlan RK Jr, Fidelman NA, *et al.* Hepatocellular carcinoma: regional therapy with a magnetic targeted carrier bound to doxorubicin in a dual MR imaging/ conventional angiography suite-initial experience with four patients. *Radiology* 2004; 230: 287-93.
- [147] Widder KJ, Senyei AE, Ranney DF. Magnetically responsive microspheres and other carriers for the biophysical targeting of anti-tumor agents. *Adv Pharmacol Chemother* 1979; 16: 213-71.
- [148] Alexiou C, Jurgons R, Schmid RJ, *et al.* Magnetic drug targeting: Biodistribution of the magnetic carrier and the chemotherapeutic agent mitoxantrone after locoregional cancer treatment. *J. Drug Targeting* 2003; 11: 139-49.
- [149] Grief AD, Richardson G. Mathematical modelling of magnetically targeted drug delivery. *J Magn Magn Mater* 2005; 293: 455-63.
- [150] Rosengart AJ, Kaminski MD, Chen H, Caviness PL, Ebner AD, Ritter JA. Magnetizable implants and functionalized magnetic carriers: A novel approach for noninvasive yet targeted drug delivery. *J. Magn. Magn. Mater* 2005; 293: 633-8.
- [151] Kubo T, Sugita T, Shimose S, Nitta Y, Ikuta Y, Murakami T. Targeted delivery of anticancer drugs with intravenously administered magnetic liposomes in osteosarcoma-bearing hamsters. *Int J Oncol* 2000; 17: 309-15.
- [152] Forbes ZG, Yellen BB, Halverson DS, Fridman G, Barbee KA, Friedman G. Validation of high gradient magnetic field based drug delivery to magnetizable implants under flow. *IEEE Trans Biomed Eng* 2008; 55: 643-9.
- [153] Yellen BB, Forbes ZG, Halverson DS, *et al.* Targeted drug delivery to magnetic implants for therapeutic applications. *J Magn Magn Mater* 2005; 293: 647-54.
- [154] Lübke AS, Bergemann C, Huhnt W, *et al.* Preclinical experiences with magnetic drug targeting: tolerance and efficacy. *Cancer Res* 1996; 56: 4694-701.
- [155] Lübke AS, Bergemann C, Riess H, *et al.* Clinical experiences with magnetic drug targeting: a phase I study with 4'-epidoxorubicin in 14 patients with advanced solid tumors. *Cancer Res* 1996; 56: 4686-93.
- [156] Inada Y, Ohwada K, Yoshimoto T, *et al.* Fibrinolysis by urokinase endowed with magnetic property. *Biochem Biophys Res Commun* 1987; 148: 392-6.
- [157] Vironchatapan E, Ueno M, Sato H, *et al.* Preparation and characterization of dextran magnetite-incorporated thermosensitive liposomes: An on-line flow system for quantifying magnetic responsiveness. *Pharm Res* 1995; 12: 1176-83.
- [158] Tam KY, Leung KC, Wang YX. Chemoembolization agents for cancer treatment. *Eur J Pharm Sci* 2011; 44: 1-10.
- [159] Wang YX. Transcatheter embolisation therapy in liver cancer. *Recent Patents on Medical Imaging* 2012; 2: 150-162.
- [160] Goldberg SN, Gazelle GS, Mueller PR. Thermal ablation therapy for focal malignancy: a unified approach to underlying principles, techniques, and diagnostic imaging guidance. *AJR Am J Roentgenol* 2000; 174: 323-31.
- [161] Jang B, Park S, Kang SH, *et al.* Gold nanorods for target selective SPECT/CT imaging and photothermal therapy *in vivo*. *Quant Imaging Med Surg* 2012; 2: 1-11.
- [162] Atsumi T, Jeyadevan B, Sato Y, Tohji K. Fundamental studies of hyperthermia using magnetic particles as thermoseeds 1: Development of magnetic particles suitable for hyperthermia. *J. Magn. Soc. Jpn* 2006;30: 555-60.
- [163] Ito A, Tanaka K, Honda H, Abe S, Yamaguchi H, Kobayashi T. Complete regression of mouse mammary carcinoma with a size greater than 15 mm by frequent repeated hyperthermia using magnetite nanoparticles. *J. Biosci. Bioeng* 2003; 96: 364-9.
- [164] Shinkai M, Suzuki M, Iijima S, Kobayashi T. Antibodyconjugated magnetoliposomes for targeting cancer cells and their application in hyperthermia. *Biotechnol. Appl. Biochem* 1994; 21: 125-37.
- [165] Shinkai M, Le B, Honda H, *et al.* Targeting hyperthermia for renal cell carcinoma using human MN antigen-specific magnetoliposomes. *Jpn. J. Cancer Res* 2001 92: 1138-45.
- [166] Ito A, Kuga Y, Honda H, *et al.* Magnetite nanoparticle-loaded anti-HER2 immunoliposomes for combination of antibody therapy with hyperthermia. *Cancer Lett* 2004; 212: 167-75.
- [167] Laurent S, Dutz S, Häfeli UO, Mahmoudi M. Magnetic fluid hyperthermia: focus on superparamagnetic iron oxide nanoparticles. *Adv Colloid Interface Sci* 2011; 166: 8-23.
- [168] Yanase M, Shinkai M, Honda H, *et al.* Antitumor immunity induction by intracellular hyperthermia using magnetite cationic liposomes. *Jpn. J. Cancer Res* 1998;89: 775-82.
- [169] Ballauff M, Lu Y. 'Smart nanoparticles': preparation, characterization and applications. *Polymer* 2007; 48: 1815-23.
- [170] Johannsen M, Gneveckow U, Eckelt L, *et al.* Clinical hyperthermia of prostate cancer using magnetic nanoparticles: Presentation of a new interstitial technique. *Int. J. Hyperthermia* 2005; 21: 637-47.
- [171] Moroz P, Jones SK, Winter J, Gray BN. Targeting liver tumours with hyperthermia: ferromagnetic embolization in a rabbit liver tumour model. *J. Surg. Oncol* 2001; 78: 22-9.
- [172] Moroz P, Metcalf C, Gray BN. Histologic analysis of liver tissue following hepatic arterial infusion of ferromagnetic particles in a rabbit liver tumour model. *Biomaterials* 2003; 24: 455-64.
- [173] Moroz P, Jones SK, Metcalf C, Gray BN. Hepatic clearance of arterially infused ferromagnetic particles. *Int. J. Hyperthermia* 2003; 19: 23-34.
- [174] Dobson J. Magnetic nanoparticle-based gene delivery. *Gene Therapy* 2006; 13: 283-7.
- [175] Mah C, Fraites TJ Jr, Zolotukhin I, *et al.* Improved method of recombinant AAV2 delivery for systemic targeted gene therapy. *Mol. Therapy* 2002; 6: 106-12.
- [176] Plank C, Schillinger U, Scherer F, *et al.* The magnetofection method: Using magnetic force to enhance gene delivery. *Biol. Chem* 2003; 384: 737-47.
- [177] Kalish H, Arbab AS, Miller BR, *et al.* Combination of transfection agents and magnetic resonance contrast agents for cellular imaging: Relationship between relaxivities, electrostatic forces, and chemical composition. *Magn Reson Med* 2003; 50: 275-82.
- [178] Wang P, Yigit MV, Medarova Z, *et al.* Combined small interfering RNA therapy and *in vivo* magnetic resonance imaging in islet transplantation. *Diabetes* 2011; 60: 565-71.
- [179] Wang P, Yigit MV, Ran C, *et al.* A theranostic small interfering RNA nanoprobe protects pancreatic islet grafts from adoptively transferred immune rejection. *Diabetes* 2012; 61: 3247-54.
- [180] Lu G, Liu PC, Poon WS, *et al.* Magnetic targeted transcatheter SPIO labeled stem cell delivery: preliminary results in a rat intracerebral hemorrhage model. *Proceedings of the European Society for Magnetic Resonance in Medicine and Biology, Antalya* 2009: No. 299.
- [181] Cheng K, Li TS, Malliaras K, Davis DR, Zhang Y, Marbán E. Magnetic targeting enhances engraftment and functional benefit of iron-labeled cardiosphere-derived cells in myocardial infarction. *Circ Res* 2010; 106: 1570-81.

- [182] Wang YX, Wang DW, Zhu XM, Zhao F, Leung KC. Carbon coated superparamagnetic iron oxide nanoparticles for sentinel lymph nodes mapping. *Quant Imaging Med Surg* 2012; 2: 53-6.
- [183] Cartmell SH, Dobson J, Verschueren SB, El Haj AJ. Development of magnetic particle techniques for long term culture of bone cells with intermittent mechanical activation. *IEEE Trans. NanoBiosci* 2002; 1: 92-7.
- [184] Dobson J, Cartmell SH, Keramane A, El Haj AJ. Principles and design of a novel magnetic force mechanical conditioning Bioreactor for tissue engineering, stem cell conditioning, and dynamic *in vitro* screening. *IEEE Trans. NanoBiosci* 2006; 5: 173-7.
- [185] Hughes S, McBain S, Dobson J, El Haj AJ. Selective activation of mechanosensitive ion channels using magnetic particles. *J. Roy. Soc. Interface* 2008; 5: 855-63.
- [186] Lin MM, Kim do K, El Haj AJ, Dobson J. Development of superparamagnetic iron oxide nanoparticles (SPIONS) for translation to clinical applications. *IEEE Trans Nanobioscience* 2008; 7: 298-305.
- [187] Ito A, Takizawa Y, Honda H, *et al.* Tissue engineering using magnetite nanoparticles and magnetic force: Heterotypic layers of co-cultured hepatocytes and endothelial cells. *Tissue Eng* 2004; 10: 833-40.
- [188] Ito A, Ino K, Hayashida M, *et al.* Novel methodology for fabrication of tissue-engineered tubular constructs using magnetite nanoparticles and magnetic force. *Tissue Eng* 2005; 11: 1553-61.
- [189] Kelkar SS, Reineke TM. Theranostics: combining imaging and therapy. *Bioconjugate Chem* 2011; 22: 1879-1903.
- [190] Khurana A, Nejadnik H, Gawande R, *et al.* Intravenous ferumoxytol allows noninvasive MR imaging monitoring of macrophage migration into stem cell transplants. *Radiology* 2012; 264: 803-11.
- [191] Bulte JW. Science to practice: can macrophage infiltration serve as a surrogate marker for stem cell viability? *Radiology* 2012; 264: 619-20.
- [192] Halamoda Kenzaoui B, Chapuis Bernasconi C, Guney-Ayra S, Juillerat-Jeanneret L. Induction of oxidative stress, lysosome activation and autophagy by nanoparticles in human brain-derived endothelial cells. *Biochem J* 2012; 441: 813-21.
- [193] Miller I, Ashton-Chess J, Spolders H, *et al.* Market access challenges in the EU for high medical value diagnostic tests. *Personalized Med* 2011; 8: 137-48.
- [194] Wang YX, Deng M. Medical imaging in new drug clinical development. *J Thorac Dis* 2010; 2: 245-52.
- [195] Wang YX. Medical imaging in pharmaceutical clinical trials: what radiologists should know. *Clin Radiol* 2005; 60: 1051-7.
- [196] Kelloff GJ, Sigman CC. Cancer biomarkers: selecting the right drug for the right patient. *Nature Reviews Drug* 2012; 11: 201-14

Received: January 31, 2013

Accepted: April 22, 2013